Slow-moving rock glaciers in marginal periglacial environment of Southern Carpathians

Alexandru Onaca[1,2], Flavius Sîrbu[2], Valentin Poncoş[3], Christin Hilbich[4], Tazio Strozzi[5], Petru Urdea[1,2]
Răzvan Popescu[6], Oana Berzescu[2], Bernd Etzelmüller[7], Alfred Vespremeanu-Stroe[6], Mirela Vasile[8],
Delia Teleagă[3], Dan Birtaş[3], Iosif Lopătiţă[1], Simon Filhol[7], Alexandru Hegyi[2,7], Florina Ardelean[1]

[1]Department of Geography, West University of Timișoara, Timișoara, Romania
[2]Institute for Advanced Environmental Research, West University of Timișoara, Timișoara, Romania
[3]Terrasigna, Bucharest, Romania
[4]Department of Geosciences, University of Fribourg, Fribourg, Switzerland
[5]Gamma Remote Sensing, Gümligen, Switzerland
[6]Faculty of Geography, University of Bucharest, Bucharest, Romania
[7]Department of Geosciences, University of Oslo, Oslo, Norway
[8]Division of Earth, Environmental and Life Sciences, University of Bucharest Research Institute, Bucharest, Romania

Correspondence to: Flavius Sîrbu (flavius.sirbu@e-uvt.ro)

Abstract. Rock glaciers, composed of debris and ice, are widely distributed across cold mountain regions worldwide. Although research on rock glaciers is gaining momentum, the distinct behaviour of rock glaciers in the marginal periglacial environments remains poorly understood. In this study, we combine remote sensing and in situ methods to gain insights into the characteristics of transitional rock glaciers in the Carpathian Mountains. We applied Persistent Scatterer Interferometry (PSInSAR) to Sentinel-1 images from 2015 to 2020 to identify areas with slope movements associated with rock glaciers and differential GNSS measurements (2019-2021) to detect the horizontal movement of 25 survey markers. Continuous ground temperature monitoring and measurements of the bottom temperature of the winter snow cover were used to examine the energy exchange fluxes characteristics of transitional rock glaciers in the Carpathians. The subsurface of one transitional rock glacier was investigated using geophysical measurements (electrical resistivity tomography and refraction seismic tomography), while petrophysical joint inversion was used to quantify the ice content. The PSInSAR methodology identified 92 moving areas (MAs) with low displacement rates (< 5 cm yr^{-1}). These MAs were generally located between 2000 and 2300 meters where solar radiation was minimal. Near-surface thermal measurements on four rock glaciers indicate favorable conditions for permafrost persistence, largely driven by internal ventilation processes (e.g., advection heat fluxes) throughout the winter. Very low ground surface temperatures were detected by BTS measurements over much of the investigated rock glaciers, particularly in their upper parts and within the MAs. Geophysical investigations reveal remnants of ice-poor permafrost within the Galeșu rock glacier, while petrophysical joint inversion modelling indicates a low ground ice content (~ 18 %) in its upper sector. At this site, the recorded surface displacements ~~are more likely the~~ result ~~of~~ from deformation within

33 the active layer and are ~~ice-melt-induced subsidence, solifluction, or the tilting and sliding of blocks within the active layer~~not

34 related to permafrost creep. The flow direction of dGNSS markers at two other rock glaciers indicated consistent movement

35 toward their fronts, a pattern typical of permafrost creep. Regarding activity status, the majority of rock glaciers in the Retezat

36 Mountains were categorized as relict, with only 21% classified as transitional. Compared to relict rock glaciers, transitional

37 ones are situated at a median elevation 150 m higher and have a slightly smaller median size.

1 Introduction

39 Rock glaciers are prominent landforms in the periglacial environment, serving as indicators of permafrost presence at the time

40 of their formation (Haeberli et al., 2006). Generated through past or present permafrost creep, they are debris-dominated

41 features typically identified by their front, lateral margins and occasionally ridge-and-furrow surface patterns (RGIK, 2023a).

42 The geomorphic imprint of permafrost creep is often preserved even after the ice within the rock glacier has completely melted

43 (Kellerer-Pirklbauer et al., 2022). In the Southern Carpathians, rock glaciers mostly present as relict landforms, yet retain

44 isolated permafrost in certain areas (Vespremeanu-Stroe et al., 2012; Onaca et al., 2013, 2015; Popescu et al., 2015, 2024).

45 Indicators such as extensive lichen cover, vegetated fronts and the overall morphological stability of many landforms suggest

46 that permafrost creep is significantly reduced compared to the colder climatic conditions of the pre-Holocene (Popescu et al.,

47 2017). These rock glaciers are predominantly mantled by angular, coarse-grained blocks which facilitate ground cooling

48 (Onaca et al., 2017a). The thermal offset associated with this blocky surface layer contributes to the maintenance of subzero

49 temperatures in the subsurface over prolonged periods (Kellerer-Pirklbauer, 2019), thereby enhancing permafrost preservation

50 even at relatively low altitudes (Colucci et al., 2019). In addition, the `chimney effect` - an advective heat flux process

51 (Delaloye and Lambiel, 2005) - significantly contributes to surface cooling in highly porous, openwork structures.

52 Permafrost creep encompasses both the internal deformation of ice within the frozen material and shearing at discrete planes

53 within or just beneath the frozen structure (Cicoira et al., 2021). Surface displacement can also result from processes occurring

54 within the active layer, such as ~~ice-melt-induced subsidence,~~ solifluction, or the tilting and sliding of blocks, which may act

55 independently of or in addition to permafrost creep (Serrano et al., 2010; Cicoira et al., 2021). The surface kinematics of rock

56 glaciers had garnered significant interest from the international community in recent years (Kellerer-Pirklbauer et al., 2024;

57 Kääb and Røste, 2024; Pellet et al., 2024; Hu et al., 2025) due to the growing need to better understand how mountain

58 permafrost responds to ongoing climate change. While the response of rock glaciers to present-day air temperature rising is

59 intricate in many instances, increased rock glacier velocities ~~has~~ have been linked to warmer climate (Wirz et al., 2016; Cicoira

60 et al., 2019; Kenner et al., 2019; Kääb et al., 2021; Marcer et al., 2021; Kellerer-Pirklbauer et al., 2024). Rising temperatures

61 within frozen debris enhance movement rates, as warming reduces the viscosity of the ice and promotes additional lubrication

62 from infiltrating water (Kääb et al., 2007). ~~According to Necsoiu et al. (2016), slow-moving rock glaciers in the Southern~~

63 ~~Carpathians exhibited increased velocities between 2007 and 2014, attributed to rising permafrost temperatures.~~ Annual rates

64 of horizontal surface kinematics of rock glaciers range from a few millimetres to a few meters (Strozzi et al., 2020), though

destabilization can result in velocities exceeding ten meters per year (Roer et al., 2008; Delaloye et al., 2013; Eriksen et al., 2018; Marcer et al., 2021; Hartl et al., 2023). Destabilization typically involves a sudden, pronounced acceleration of a section of the rock glacier, with displacement rates increasing by up to two orders of magnitude and surface manifestations such as cracks, scarps, and crevasses reflecting enhanced internal strain between stable and unstable areas (Marcer et al., 2021; Hartl et al., 2023).

Many studies have demonstrated the feasibility of satellite radar interferometry (InSAR) for kinematic analysis of rock glaciers, capable of detecting motion at the millimetre scale (Liu et al., 2013; Necsoiu et al., 2016; Strozzi et al., 2020; Bertone et al., 2022). This technique enables the mapping of land surface deformation with an appropriate spatial and temporal resolution over vast areas (Bertone et al., 2022). Surface displacements can be attributed to permafrost creep only if the flow direction and velocity remain spatially consistent and uniform over a documented period (RGIK, 2023a). Permafrost creep typically occurs when the thickness of the ice-rich core in rock glaciers reaches at least 10-25 m (Cicoira et al., 2021). In contrast, displacements observed in rock glaciers with thinner layers of frozen debris are primarily driven by deformations within the active layer above the permafrost table.

While rock glaciers in discontinuous permafrost have been extensively studied, the distinctive behaviour of those in marginal periglacial environments has received far less attention (Serrano et al., 2010; Necsoiu et al., 2016). In such settings, rock glaciers exhibit ~~either no movement or~~ significantly slower movement rates (a few cm yr^{-1}) and are often referred to as transitional rock glaciers (RGIK, 2023a). This reduced surface velocity is attributed to the high shear strength of the material, which inhibits fast creep movement (Cicoira et al., 2021). Even if slow-moving rock glaciers were documented in various regions of the world (Brencher et al., 2021; Bertone et al., 2022; Lilleøren et al., 2022; Lambiel et al., 2023), the relationship between their velocity and ground ice content was rarely addressed (Serrano et al., 2010). Since borehole information is limited in high and remote mountains, a promising alternative to quantitatively estimate ground ice content is using petrophysical joint inversion (PJI) of seismic refraction and electrical resistivity data (Wagner et al., 2019).

The Southern Carpathian range is a key region in Europe where transitional rock glaciers are studied. Here, the enhanced continentality effects induce a distinct pattern of manifestation of periglacial phenomena compared with other mid-latitude mountains in Europe (Onaca et al., 2017a). In marginal periglacial mountains, permafrost occurrence is generally sporadic or patchy and site-specific characteristics highly control its distribution (Stiegler et al., 2014; Onaca et al., 2015; Kellerer-Pirklbauer, 2019; Popescu et al., 2024). ~~Above 2000 m in the Southern Carpathians, the 1991-2020 climatological period was 0.8 ºC warmer than the 1961-1990 baseline (Berzescu et al., 2025).~~

The paper aims to present new results on the rock glaciers ~~dynamics~~ kinematics and permafrost characteristics in the Retezat Mountains and, more ~~broadly~~precisely, to better understand the behaviour of rock glaciers in marginal periglacial mountains. To achieve this goal, we will (i) locate and assess the kinematics of rock glaciers` moving areas using SAR-based persistent scatterers interferometry (PSInSAR); (ii) update the existing rock glacier inventory in the Retezat Mountains with information on the rock glacier kinematics~~dynamics~~; (iii) estimate ground ice content using petrophysical joint inversion based on electrical resistivity and seismic refraction data and (iv) characterise the thermal conditions at the rock glaciers surface.

2. Study area

The Retezat Mountains are among the highest massifs in the Romanian Carpathians, constituting a distinct part of the Southern Carpathians (the latter are also known as the Transylvanian Alps). Located in the western part of the Southern Carpathians (45°22' N and 22°53' E), the Retezat Mountains reach an elevation of 2500 m, revealing a typical alpine landscape (Fig. 1). The climate in this region can be characterised as a moderate temperate continental climate, classified within the subarctic or boreal category according to the Köppen classification system. Between 2000 and 2100 m elevation, the mean annual air temperature is approximately 0° C, annual precipitation averaging around 1000 mm (calculated for the period 1961-2007) (Onaca et al., 2017a). Above 2000 m in the Southern Carpathians, the 1991-2020 climatological period was 0.8 ºC warmer than the 1961-1990 baseline (Berzescu et al., 2025).

The mountain range is part of the orogenic units spanning two distinctive tectonic-structural regions: the Danubian Domain and the Getic Domain, both with the status of a thrust sheet. The Danubian Domain, referred to as the Danubian Autochtonous, is primarily characterised by two dominant granitic bodies, Retezat and Buta (Pavelescu, 1953). These granitic bodies are surrounded in the marginal area by epi- and meso-metamorphic schists, typifying the Getic Nappe. Specific Mesozoic rocks, particularly limestones, are prevalent in the southern part of this mountain range (Urdea, 2000). 87 % of the rock glaciers in the Retezat Mountains have developed on granite bedrock (Fig. 2), while the remaining landforms are situated on metamorphic schists.

The Retezat Mountains boast one of the most comprehensive and distinct arrays of glacial and periglacial landforms in the Romanian Carpathians. Notably, they host the largest glacial cirques in the Romanian Carpathians, with a combined area of

117 all glacial cirques amounting to c. 8 % of the massif's total area (Urdea, 2000). During the Last Glacial Maximum (LGM) (20.6
118 ka), glaciers in these mountains reached lower elevations ranging from 1000 to 1300 m (Ruszkiczay-Rüdiger et al., 2021).

119
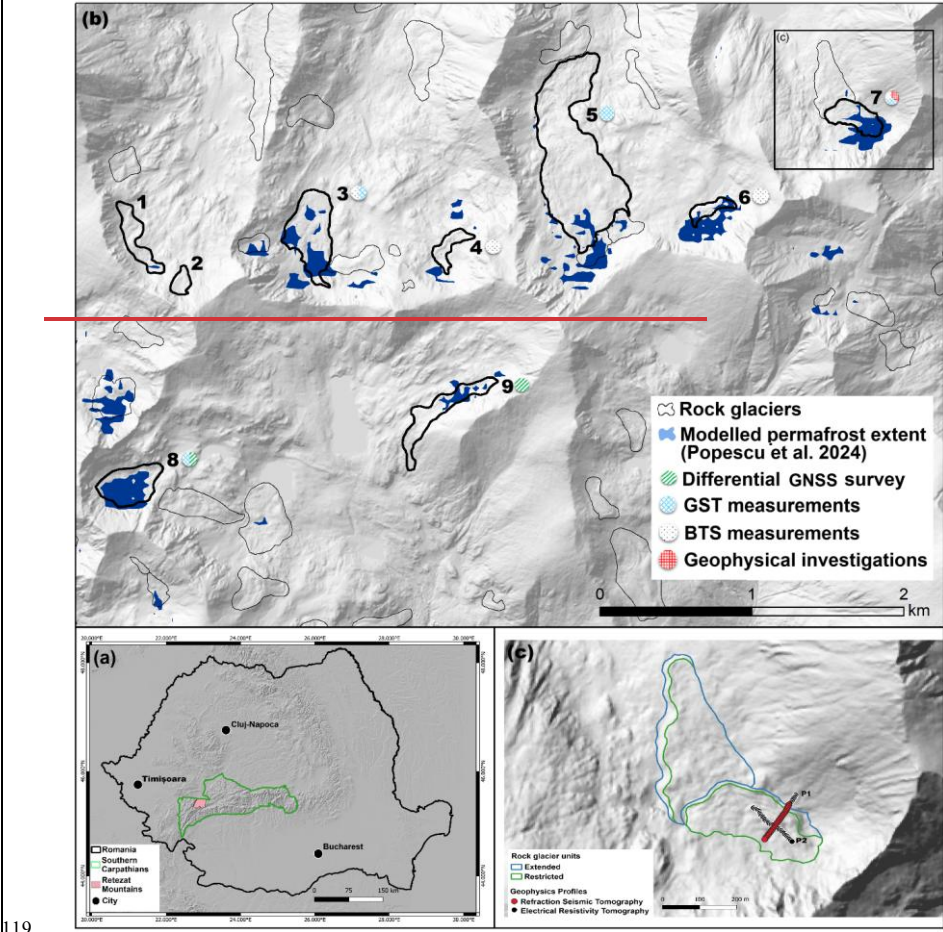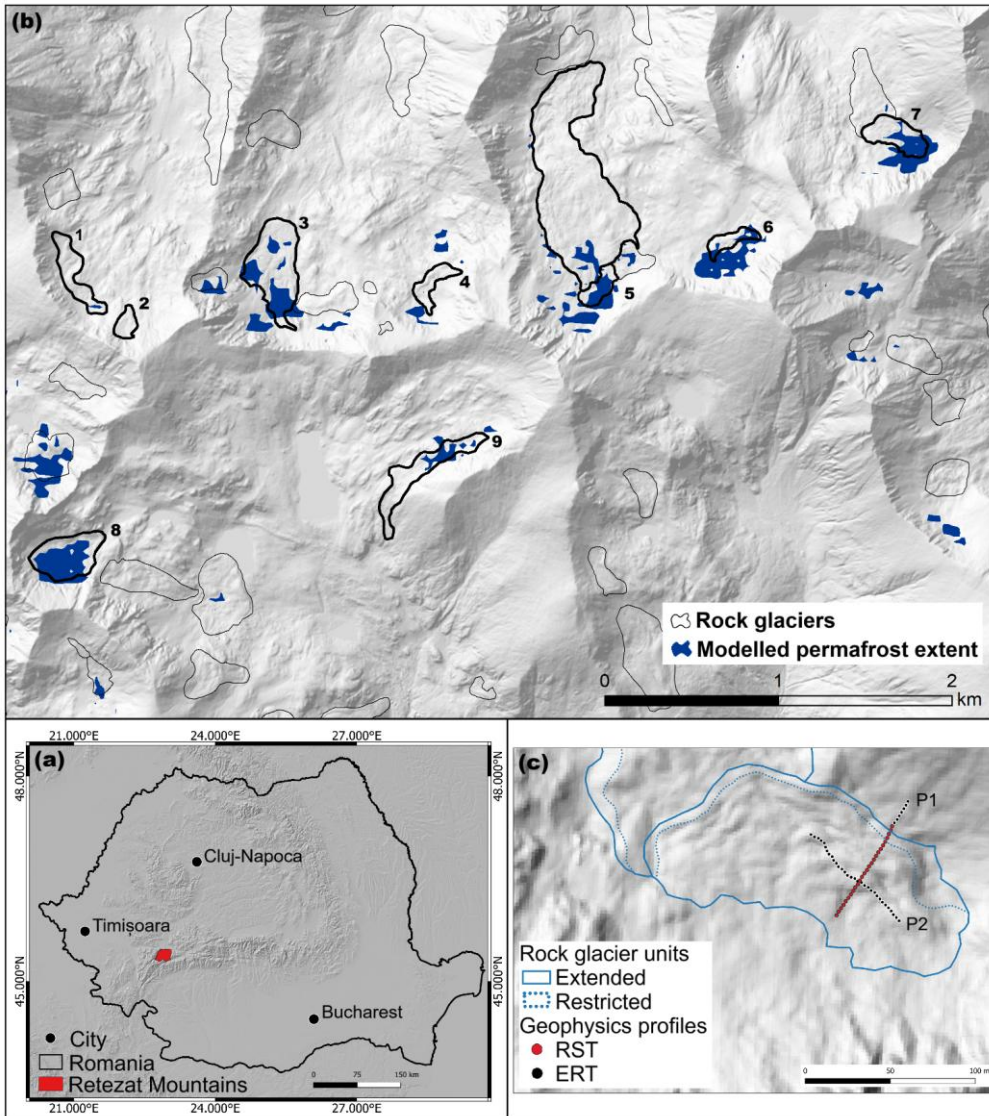
Figure 1: Study sites. (a) Overview map with the location of the Retezat Mountains ~~in the Southern Carpathians and~~ **in Romania, background of the map: hillshade based on FABDEM (Howker et al. 2022). (b) modelled permafrost extent (Popescu et al., 2024) and spatial distribution of rock glaciers in the Retezat Mountains overlaid on a hillshade based on the LAKI II DEM (LAKI II MNT, 2024). The rock glaciers that are discussed in the present paper** are mapped with thicker lines and ~~are numbered (1 - Stânişoara, 2 - Bucura, 3 - Pietrele, 4 - Pietricelele, 5 - Valea Rea, 6 - Păpuşa, 7 - Galeşu, 8 - Judele, 9 - Berbecilor), and the ground based measurements that have been performed on each of them are represented by a composite symbol near the number~~are presented in Table 1. **(c) A detailed map with the position of the geophysics profiles on Galeşu rock glacier; note: same background image as (b).**

Table 1. Rock glaciers investigated through ground-based measurements and/or discussed in this study (BTS = bottom temperature of snow cover; GST = ground surface temperatures ERT = electrical resistivity tomography; RST = refraction seismic tomography, dGNSS = differential GNSS measurements).

Number in Fig.1	RG name	RG activity	Ground-based measurements type
1	Stânişoara	Relict	-
2	Bucura	Transitional	-
3	Pietrele	Relict	BTS, GST
4	Pietricelele	Transitional	BTS
5	Valea Rea	Relict	GST
6	Păpuşa	Transitional	BTS
7	Galeşu	Transitional	BTS, GST, ERT, RST
8	Judele	Transitional	GST, dGNSS
9	Berbecilor	Transitional	dGNSS

Subsequently, the Late Glacial period witnessed five phases of deglaciation. However, no glacial advance has been documented in the central part of the Retezat Mountains during or after the Younger Dryas based on cosmic-ray exposure dating (Ruszkiczay-Rüdiger et al., 2021). Rock glaciers in the Retezat Mountains likely began to develop during the Younger Dryas, with most having become relict or transitional since the onset of the Holocene. Permafrost associated with rock glaciers had been documented since 1993 in this mountain range (Urdea, 1993). A recent inventory described Retezat Mountains as the range with the highest number (94) and density (0.52 landforms/km^2, and 2.87 ha/km^2 at altitudes above 1540 meters) of

149 rock glaciers in the Romanian Carpathians (Onaca et al., 2017b) (Fig. 1). Additionally, they harbour the longest Carpathian

150 rock glacier, Valea Rea, extending 1.4 km (Urdea, 2000) (Fig. 2b).

151 According to Necsoiu et al. (2016), slow-moving rock glaciers in the Southern Carpathians exhibited increased velocities

152 between 2007 and 2014, attributed to rising permafrost temperatures. They exhibited a velocity rise of 20% between 2007 and

153 2014.

154
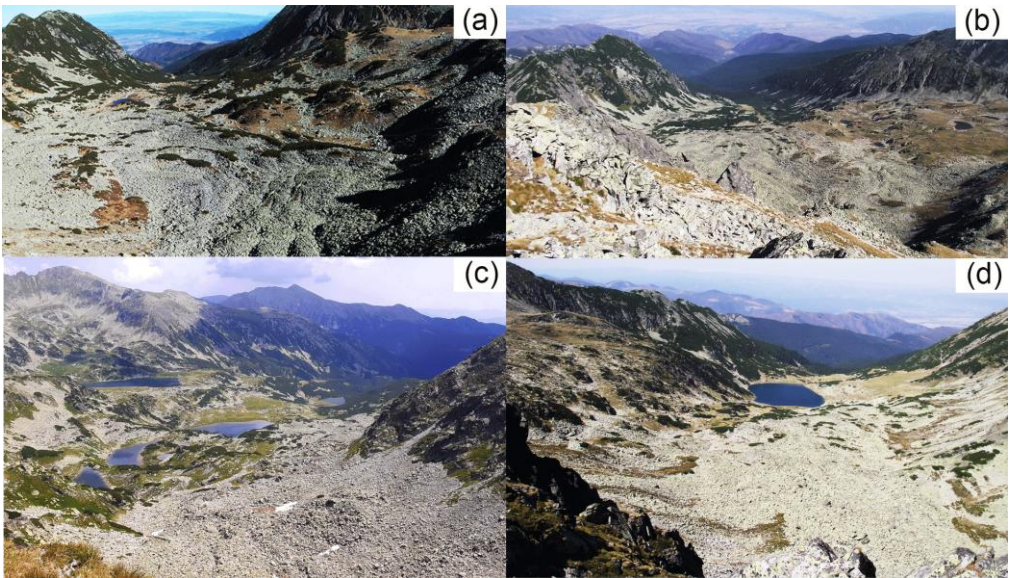
Figure 2: Pictures of rock glaciers from Retezat Mountains: a) Pietrele (3) – relict; b) Valea Rea (5) – transitional; c) Judele (8) – transitional; d) Galeșu (7) – relict. Photo credit: A. Onaca. ~~Pictures of the rock glaciers in the Retezat Mountains: , (a) Pietrele; (b) Valea Rea; (c) Judele; (d) Galeșu.~~ **Photo credit: A. Onaca.**

3. Methods

3.1. Rock glacier inventory

160 Rock glaciers are categorised into three types based on their activity status: active, transitional, or relict, as outlined by (RGIK,

161 2023a). Active rock glaciers exhibit consistent downslope movement across most of their surface with displacement rates

162 ranging from a decimetre to several meters per year (RGIK, 2023a). Most of the surface of a transitional rock glacier

163 experiences little to no downslope movement, with annual average displacement rates generally falling below one decimetre

164 (RGIK, 2023a). Rock glaciers exhibiting no detectable movement across most of their surface are classified as relict (RGIK,

165 2023a).

166 This study revised the existing inventory of rock glaciers in the Southern Carpathians (Onaca et al., 2017b) in accordance with
167 the guidelines provided by RGIK (2023a). The inventory involved mapping rock glaciers through fieldwork surveys and
168 detailed examination of high-resolution aerial imagery. Due to the availability of kinematic information for only a limited
169 number of landforms (Vespremeanu-Stroe et al., 2012; Necsoiu et al., 2016), the current inventory lacks data on the activity
170 of rock glaciers. Information on rock glacier kinematics was only available for a few landforms (Vespremeanu-Stroe et al.,
171 2012; Necsoiu et al., 2016), while most of the rock glaciers were classified as either intact or relict based on geomorphological
172 and ecological criteria (e.g., degree and type of vegetation cover).

3.2. Persistent scatterer interferometry using Sentinel-1 data

174 PSInSAR is a remote sensing technique designed to measure ground displacements along the radar line of sight (SAR LOS)
175 with millimetric accuracies (Rucci et al., 2012; Yu et al., 2020). Although Sentinel-1 (S1) SAR data does not offer the highest
176 possible spatial resolution, its worldwide periodic coverage and open data policy has enabled wide-scale monitoring since
177 2014, leading to a thriving archive of ground-motion products with various applications.
178 Sentinel-1 serves as the backbone of the operational PSInSAR application development for the European Ground Motion
179 Service (EGMS), openly available throughout the entire European area. The PSInSAR analysis employed in this study was
180 developed by Terrasigna and generally follows the EGMS specifications (https://land.copernicus.eu/en/technical-library/egms-
181 algorithm-theoretical-basis-document/@@download/file)(EEA, 2025). However, there are a few differences, particularly
182 related to the choice of reference points, the modelling of atmospheric effects in steep terrain and the selection of SAR images.
183 EGMS products are computed at the regional level, where reference points are typically located in lowland areas covered by
184 infrastructure, which provides strong and stable radar backscattering. Additionally, EGMS includes all available acquisitions,
185 even those affected by snow cover at high altitudes. However, inspection of EGMS products reveals that extending the
186 measurement network from lowland reference points to mountain summits was largely unsuccessful. This is mainly because
187 the atmospheric path delay associated with steep topography was not adequately compensated for and acts like phase noise.
188 Furthermore, snow cover during winter significantly impacts data quality. Non-homogeneous snow or snow with variable
189 humidity scatters radar signals and increases phase noise. If the case of dry snow, radar waves penetrate the snowpack, but
190 because they propagate more slowly than in air, the interferometric phase experiences a time delay. This delay produces
191 apparent subsidence (false ground displacement away from the radar sensor). Combined these factors often result in the
192 rejection of radar targets on mountain tops due to excessive noise.
193 To address these issues, Terrasigna carefully selected reference points located on mountain summits, where the topographic
194 atmospheric delay is similar to that of the areas of interest. Additional efforts were made to improve the accuracy of
195 atmospheric delay modelling and compensation. Furthermore, only snow-free acquisitions were considered. As a result, the
196 high density of radar targets – formed by bare rocks at the top of the mountains – is preserved in our measurements.
197 Both ascending and descending paths were processed for cross-validation, along with L-band ALOS data, which was analyzed
198 for the same purpose. Because descending passes occur in the early morning – when atmospheric conditions are generally

199 more stable than in the evening – the resulting measurements tend to be less noisy. A 2D decomposition between ascending
200 and descending passes is technically feasible; however, the steep topography introduces several challenges. First, areas that
201 are clearly visible from one orbit may be in shadow or appear foreshortened in the other, reducing data quality and spatial
202 consistency. Second, since the topography is steep, the preferential direction of ground movement is often dictated by the slope
203 of the terrain. Additionally, the 2D decomposition estimates vertical and east-west displacement components under the
204 assumption that there is no north-south movement – an assumption that is frequently invalid in mountainous regions, where
205 north-south displacement is commonly observed. Based on these issues, it was decided to use the orbits that yielded the best
206 results for validation and mapping.
207 Figure 3a illustrates the total coverage (from all available S1 paths from both the Ascending and Descending orbits) of the
208 EGMS product in the area of interest, while Figure 3b illustrates the PSInSAR analysis of the same area, derived solely from
209 one S1 path (Path 80 Descending). In the following, this is referred to as `Terrasigna PSInSAR`. It is evident that the EGMS
210 coverage is relatively sparse and does not highlight dynamic areas – there are no zones marked in red, which typically indicate
211 significant ground motion. In contrast, the PSInSAR results from Terrasigna show much denser coverage and clearly identify
212 dynamic areas, with red colors representing higher displacement rates. In general, there are technical differences in the
213 computation of data across EGMS products, primarily due to the involvement of multiple groups in the project. Terrasigna's
214 algorithms are more closely aligned with those used for the EGMS in southern Europe, which appear to offer better extraction
215 of non-linear motion.
216 In this study, the kinematics of the rock glaciers were assessed using 181 images acquired between May 15, 2015, and October
217 4, 2021, covering only the snow-free periods to avoid coherence loss. The motion was measured along the SAR LOS direction;
218 however, the actual displacement of the rock glacier surface is expected to mainly occur along the slope or in the vertical
219 direction. The PSInSAR algorithm, as described by Rucci et al. (2012), Crosetto et al. (2016) and Poncoș et al. (2022),
220 preserved all displacement information to maximize the chances of detecting slow movements (mm yr^{-1}) in areas without
221 vegetation cover. The process began by extracting linear deformation information before applying any spatial or temporal
222 filtering, which was typically used to improve phase statistics. A key challenge is that the atmospheric phase is two orders of
223 magnitude larger than the displacement signal (Poncoș et al., 2022), requiring meticulous phase unwrapping and correction of
224 each residual interferogram. Due to significant atmospheric noise in steep terrain or in areas with large elevation differences,
225 a reference point at a similar elevation to the rock glaciers was chosen on the mountain summit. This approach minimizes
226 atmospheric phase differences, improving coherence and reliability of the PSInSAR measurements. An important number of
227 rock glaciers in the area are oriented north-south or south-north, which may lead to an underestimation of the along-slope
228 actual displacements due to the limited sensitivity of the satellite look angle to slope-parallel motion.

229

230
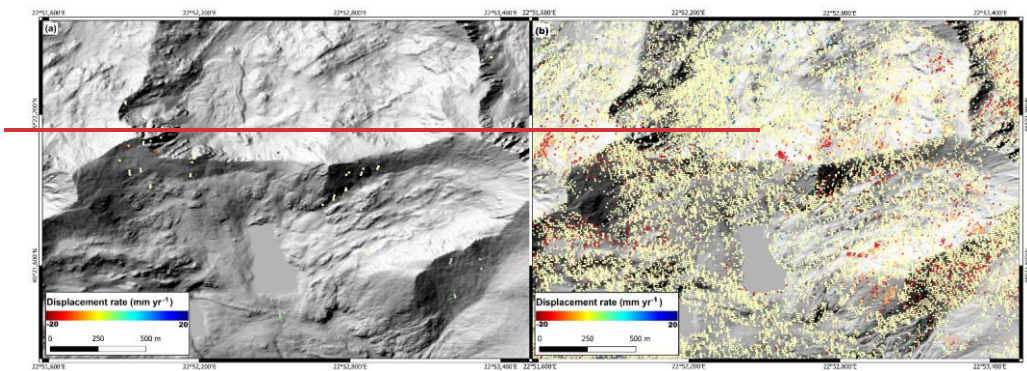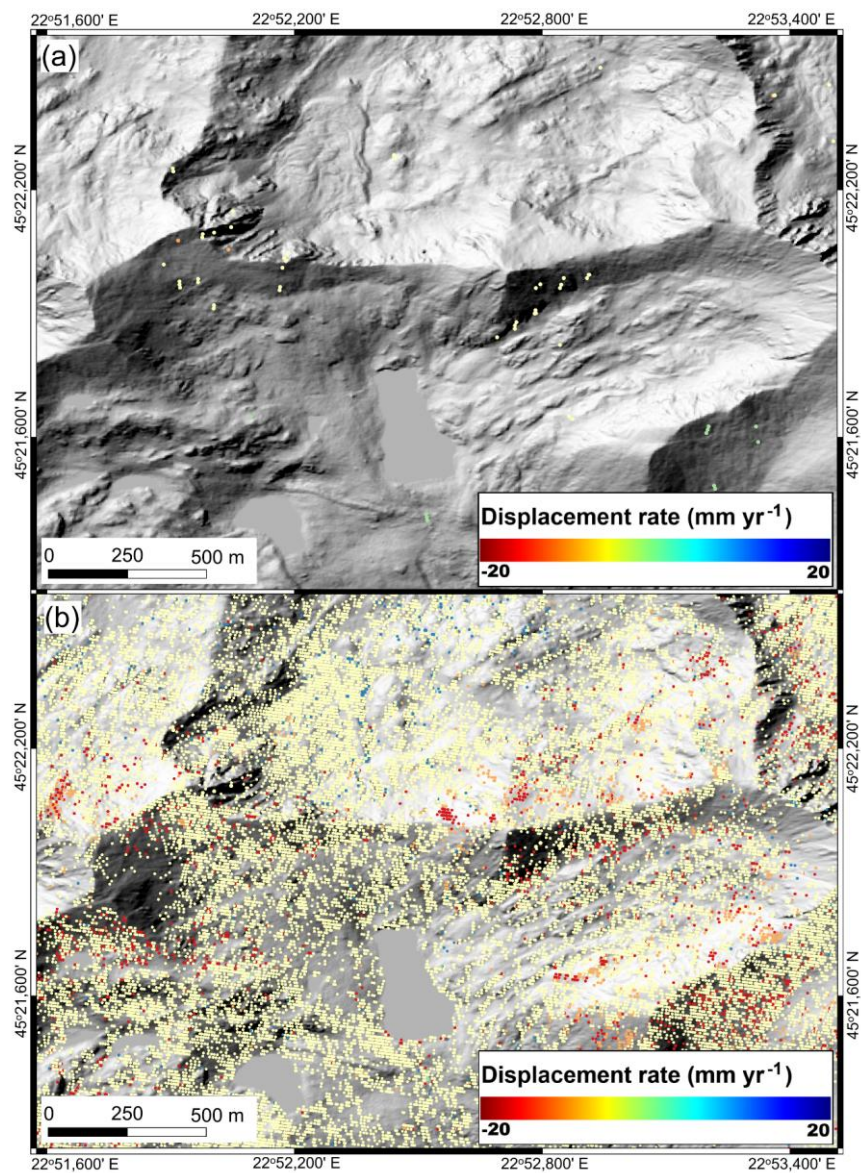
Figure 3: Comparison between the PSInSAR spatial density of measurements obtained by EGMS (a) and Terrasigna (b) in the central area of Retezat Mountains. Background of both maps: hillshade based on the LAKI II DEM (LAKI II MNT, 2024).

The PSInSAR results were analysed using the Persistent Scatterers Online Software Tool (PSTool), a web-based platform developed by Terrassigna Inc. (Poncoș et al., 2022), to exploit a large volume of ground displacement data. The PSTool platform can be used to inspect temporal characteristics of the ground motion, select areas of interest and extract temporal averages of displacement rates, export temporal profiles to standard formats for integration in the user's own platforms and upload user-specific layers on top of the displacement information.

3.3. Inventorying moving areas

According to RGIK (2023a) guidelines, a moving area (MA) represents an area at the surface of the rock glacier characterised by relatively homogeneous velocity rates and consistent flow direction. Based on multi-annual surface velocity rates, MAs were identified and delineated within the inventoried rock glaciers (Onaca et al., 2017b) using Terrasigna PSInSAR results. The next step was to assign standardised velocity classes to moving areas ~~The next step was to assign velocity classes to moving areas considering the standardised velocity classes~~ (Barboux et al., 2014; Bertone et al., 2022). In our case, MAs were attributed to one of the following SAR LOS deformation velocity classes: undefined, 0.3-1 cm yr^{-1}, 1-3 cm yr^{-1}, and 3-10 cm yr^{-1}, undefined (RGIK, 2023a) (Fig. 4). The velocity class characterizes the average yearly displacement rate recorded within a MA during the 2015-2021 period. The undefined category was assigned to MAs characterised by inhomogeneous velocity rates. PSInSAR-based surface displacement of ≤ 0.3 cm yr^{-1} were assigned to the "no movement" category, as this threshold was considered the lower limit of velocity detection on S1 interferograms in this type of approach (Rouyet et al., 2021). The moving areas were manually digitized and compiled into an inventory using ArcGIS 10.8. Since many surface displacements in marginal periglacial regions result from active layer deformations (e.g., melt-induce subsidence), we have set the minimum area for an MA at 1000 m^2 to exclude those not associated with permafrost creep. For the spatial analysis of the rock glaciers and MAs, we used a one-meter resolution digital elevation model generated from high-resolution LiDAR source data acquired in 2018 (LAKI II MNT, 2024).

Formatted: Font: (Default) Times New Roman

3.4. Differential GNSS measurements

Judele (8) and Berbecilor (9) rock glaciers had been surveyed by differential GNSS (DGNSS) measurements every summer between 2019 and 2021. A differential dual-frequency Topcon Hiper V GPS had acquired high-precision positioning data in real-time kinematics mode. The dGNSS device uses two receivers, one installed as a fixed base station, whereas the roving receiver was moved to different points of interest in the field. The mobile receiver gets the corrected position information calculated by the base station via a radio signal in order to measure a point with very high precision (i.e. < 1 cm accuracy in the horizontal plane). 25 survey markers were measured in October 2019 and remeasured in October 2020 and 2021. Two points outside the boundaries of the rock glaciers, located on stable bedrock, were also measured to assess the horizontal

262 accuracy of the DGNSS. The difference between the yearly measurements in both cases indicated an accuracy range of 0.3 to

263 0.6 mm/yr^{-1}.

264 The velocities used in the analysis were calculated between the initial and final position over a two-year period.

265 The mean DGNSS velocities used in the analysis were calculated as the yearly displacement between the initial and final

266 position over a two-year period.

3.5. Validation with ALOS-2 PALSAR-2 interferometry

268 To further validate Terrasigna's PSInSAR analysis specifically developed for this study, we considered a series of six ALOS-

269 2 PALSAR-2 images regularly acquired between 2014 and 2019 at the end of the snow-free season in September and October.

270 We computed wrapped differential interferograms with time intervals ranging from one to five years using a DEM with 10 m

271 pixel spacing obtained from 1:25 000 scale topographic maps with a contour interval of 10 m. For the interpretation of the

272 interferograms, we followed the practical guidelines of the IPA Action Group Rock glacier inventories and kinematics (RGIK,

273 2023b). We masked areas affected by geometrical distortions and used only interferograms from snow-free periods. Kinematic

274 attributes were assigned only when the signals were reliable (e.g., in descending mode). Moving areas were independently

275 identified and delineated, and then linked to the existing Rock Glacier Units (RGUs) (RGIK, 2023b).

3.6. Thermal conditions

277 The bottom temperature of the winter snow cover (BTS) is an efficient method to map permafrost distribution in non-arid

278 mountains (Vonder Mühll et al., 2002). If optimum snow conditions are met, the BTS values indicate probable permafrost at

279 < -3 ºC, possible permafrost at -2 to -3 ºC and absence of permafrost at > -2 ºC (Haeberli, 1973; Hoelzle, 1992; Popescu et al.,

280 2024). However, in dry, porous bouldery surfaces where air convection and advection occur, this method lacks the precision

281 needed to accurately map permafrost occurrence (Bernhard et al., 1998). Nevertheless, the BTS method remains highly

282 effective for distinguishing areas with colder ground surface temperatures from those with warmer ones. Two classical 2.6 m

283 long BTS probes equipped with digital thermometers (0.5 ºC precision) were used to measure 140 thermal records at the snow-

284 ground interface. The BTS measurements were acquired at the end of March 2022 on four rock glaciers in three north-facing

285 valleys in the central part of the Retezat Mountains (Fig. 1). At all the sites where BTS values were recorded, the snow was

286 sufficiently thick (> 80 cm) to insulate the ground from external air temperature fluctuations (Ishikawa et al., 2003). Previous

287 studies in the Southern Carpathians (Vespremeanu-Stroe et al., 2012; Onaca et al., 2015) revealed that in March, BTS values

288 remain nearly constant below a thick snow cover, which usually falls in November or December.

289 Minimal temperature data loggers became widely used in mountain permafrost terrain to get more detailed insights into the

290 energy exchange fluxes at the surface of rock glaciers (Hoelzle et al., 1999). Four rock glaciers in the central part of the Retezat

291 Mountains were selected to monitor the thermal regime at the ground surface (Fig. 1b). The evolution of ground surface

292 temperature (GST) was recorded using iButtons DS1922L data loggers. According to the producer, the miniature thermistors

293 used in this study have an accuracy of ± 0.5 ºC and measure temperatures between -40 and 80 ºC. The sensors were indirectly

294 calibrated at 0 ºC using the snow melting period ("zero curtain" interval), and GST data were measured and logged every 2

295 hours. In mid and late winter, the ground surface temperature remains stable under a thick insulating layer, and the subsurface

296 mainly controls the energy flux. This is why the "winter equilibrium temperature" (WEqT) is considered an excellent empirical

297 predictor of permafrost existence if temperatures are low (i.e., < -2 ºC) (Sattler et al., 2016). WEqT refers to stable ground

298 surface temperature period lasting at least two weeks, generally occurring in late winter, when snow cover exceeds 50 cm in

299 thickness (Schoeneich, 2011). WEqT and mean annual ground surface temperature (MAGST) were calculated for each GST

300 monitoring site.

3.7. Geophysical Methods and PJI Modelling

302 Geophysical methods, such as electrical resistivity tomography (ERT) and refraction seismic tomography (RST), are widely

303 applied in mountain permafrost studies and have the potential to characterise subsurface structure and heterogeneity and detect

304 and map ground ice occurrences (Hauck et al., 2011; Herring et al., 2023). Both methods are sensitive to differences between

305 frozen and unfrozen subsurface conditions. As ice can be considered an electrical insulator as opposed to water, the electrical

306 resistivity increases exponentially with decreasing temperatures below 0 °C. Similarly, the seismic P-wave velocity of ice is

307 with 3500 m s^{-1} significantly higher than that of liquid water ($\sim$ 1500 m s^{-1}) or air (330 m s^{-1}), allowing to differentiate between

308 frozen sediments (containing ice) and unfrozen sediments (pore space filled with water or air).

309 ERT is the most common geophysical technique applied in permafrost research and is used for mapping permafrost occurrence

310 where no borehole information is available, as well as monitoring changes in the ice-to-water ratio (Wagner et al., 2019;

311 Mollaret et al., 2020). The RST method is often used as a complementary method to ERT to reduce the ambiguity in the

312 interpretation of ERT data, as the P-wave velocity v_p is mainly controlled by density, and variations in v_p allow to identify

313 porosity changes, or discriminate between liquid (water) and solid (ice) pore fluid, as well as in determining the depth to the

314 bedrock.

315 In the absence of ground truth information about the state of permafrost, another advantage of geophysical data is, that co-

316 located ERT and RST data can be used to quantitatively estimate the content of the four phases (i.e., rock, ice, water and air)

317 using the so-called 4-phase model approach, which is based on the petrophysical equations by Archie (1942) for the electrical

318 resistivity and that of Timur (1968) for the P-wave velocity.

319 Recently, the approach has been further developed by Wagner et al. (2019), to the so-called petrophysical joint inversion (PJI)

320 framework, permitting the joint inversion of ERT and RST data sets to simultaneously solve for the subsurface distribution of

321 the 4 phases. The main advantage of the PJI is the increased accuracy of the parameters estimated, as the algorithms iteratively

322 search for a subsurface model that simultaneously explains the seismic and resistivity measurements. This is especially relevant

323 for the porosity model, which is represented more realistically in the PJI than in previous versions of the 4-phase model (Hauck

324 et al., 2011). Mollaret et al. (2020) demonstrated the applicability of the PJI for data collected on different alpine permafrost

325 landforms with different ice contents.

326 In the field, 2D ERT data were collected using a GEOTOM (Geolog) multi-electrode instrument equipped with 50 electrodes
327 spaced 4 meters apart. By combining a multitude of individual measurements with different electrode combinations (i.e.
328 quadrupoles) along a profile line, a 2-dimensional resistivity model of the subsurface is obtained. All measurements were
329 performed in the Wenner configuration to ensure an optimal signal-to-noise ratio, which is especially important in dry and
330 coarse-blocky terrain.
331 2-dimensional RST data were obtained using a 24-channel Geode seismometer (Geometrics). An artificial seismic wave is
332 produced by hitting a sledgehammer to the ground, and the waves travel along different paths through the subsurface and back
333 to the surface, where they are registered by 24 geophones. The subsurface structure and composition can be derived from the
334 travel time the so-called P-wave needs from the source (i.e. hammer) to the geophones. The wave velocity (v_p in m s^{-1}), and
335 thus the travel time, is basically a function of the density of the subsurface material, and the obtained seismic velocity allows
336 inferring the subsurface material. The pre-processing of the seismic field data (picking of first arrivals) was performed using
337 the software *ReflexW* (Sandmeier, 2020). The individual ERT and RST data sets were first independently inverted using the
338 PyGimLi framework (Rücker et al., 2017), and in a second step, the PJI was conducted to estimate ground ice contents using
339 the approach developed by (Wagner et al., 2019).

340 **4. Results**

341 **4.1. Inventorying moving areas**

342 In the Retezat Mountains the MAs exhibited velocities ranging from 0.3 to 5 cm yr^{-1} (Fig. 4 and 5), and were classified into
343 three velocity classes: 0.3 – 1 cm yr^{-1}, 1 – 3 cm yr^{-1}, and 3 – 10 cm yr^{-1}. The measured displacement between 2015 and 2021
344 remained consistent constant for most MAs, with no significant changes in velocity during this period (see trendlines in Fig.
345 5). Due to the relatively low velocities of the MAs, tracking seasonal variations involved high uncertainty; therefore, we
346 referred only to annual or multiannual displacement rates.
347 A total of 92 MAs covering 0.27 km^2 were inventoried in the Retezat Mountains rock glaciers. Most of the MAs are classified
348 with the slow velocity class (0.3 – 1 cm yr^{-1} and 1-3 cm yr^{-1}) (Fig. 6), while only 10 % of the MAs are characterised by velocity
349 class 3-10 cm yr^{-1} (Fig. 6a). Around one-third (37 %) of the total number of rock glaciers in the Retezat Mountains contains
350 MAs, but the analysis revealed they usually occupy only a small portion (< 30 %) of the total surface of each rock glacier; in
351 six cases, the cumulated area of MAs represents more than 50 % of the rock glacier area (Fig. 6d). The mean area of MAs is
352 0.3 ha, ranging from 0.1 to 1.77 ha.
353 The number of MAs in each rock glacier varies between 1 and 8, but in most cases (69 %), 1 to 3 MAs occur in an individual
354 RG. MAs characterised by velocities > 3 cm yr^{-1} were identified in 8 rock glaciers, whereas MAs classified in the velocity
355 class 1-3 cm yr^{-1} appear in 17 (Fig. 6c).
356 The median elevation for each MA class falls between 1950 and 2295 m (Fig. 7). Specifically, 62 % of the MAs are found in
357 the elevation band of 2100 to 2200 m, while 17 % lie between 2200 and 2295 m. Additionally, 16 % of the moving areas are

358 situated in the range of 2000 to 2100 m, and only 5 % are below 2000 m. Among these, MAs categorised under velocity classes

359 of 1-3 and 3-10 cm yr^{-1} generally occur at the highest elevations (Fig. 7a). Figure 7b illustrates the variability of slopes across

360 the MAs velocity classes, revealing mean values ranging from 8 to 42º. The widest range of slopes is observed in the velocity

361 class 0.3 – 1 cm yr^{-1}, which also exhibits higher median values. Half of the MAs (50 %) face north (Fig. 8), despite that only

362 21 % of the inventoried rock glaciers in the Retezat Mountains stand out on the northern aspects. The NE and E slopes host

363 more MAs (32 %) compared to NW and W aspects (23 %) in respect with the rock glacier distribution (Fig. 8). Across the

364 mountain range, slopes with a western aspect dominate in terms of surface coverage. The MAs with velocities exceeding 3 cm

365 yr^{-1} receive the lowest potential solar radiation (Fig. 7c).

367
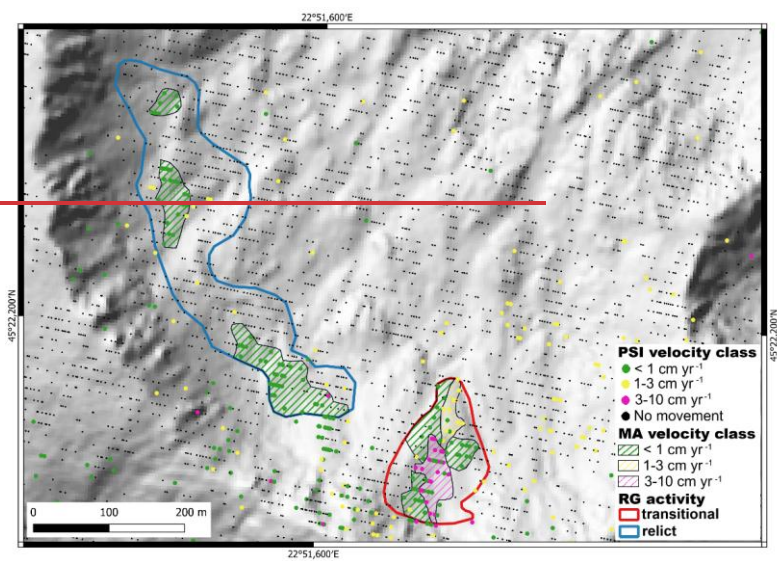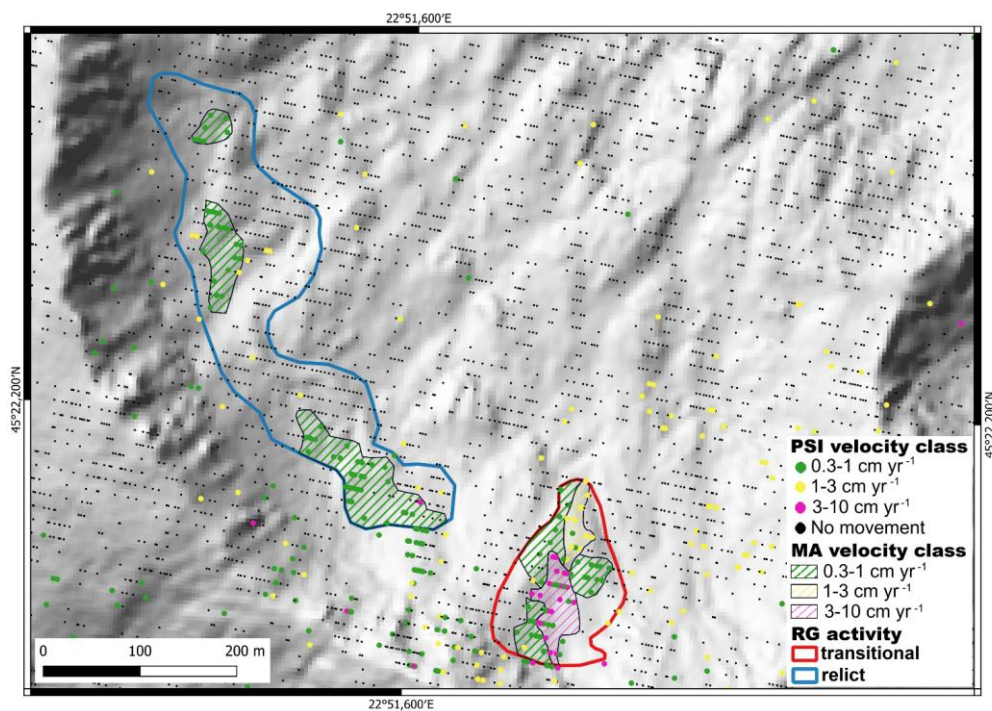
Figure 4: Example of moving areas and rock glacier activity for the Retezat Mountains. The two RGs are marked with numbers 1 and 2 in fig.1. Background image: hillshade based on the LAKI II DEM (LAKI II MNT, 2024).
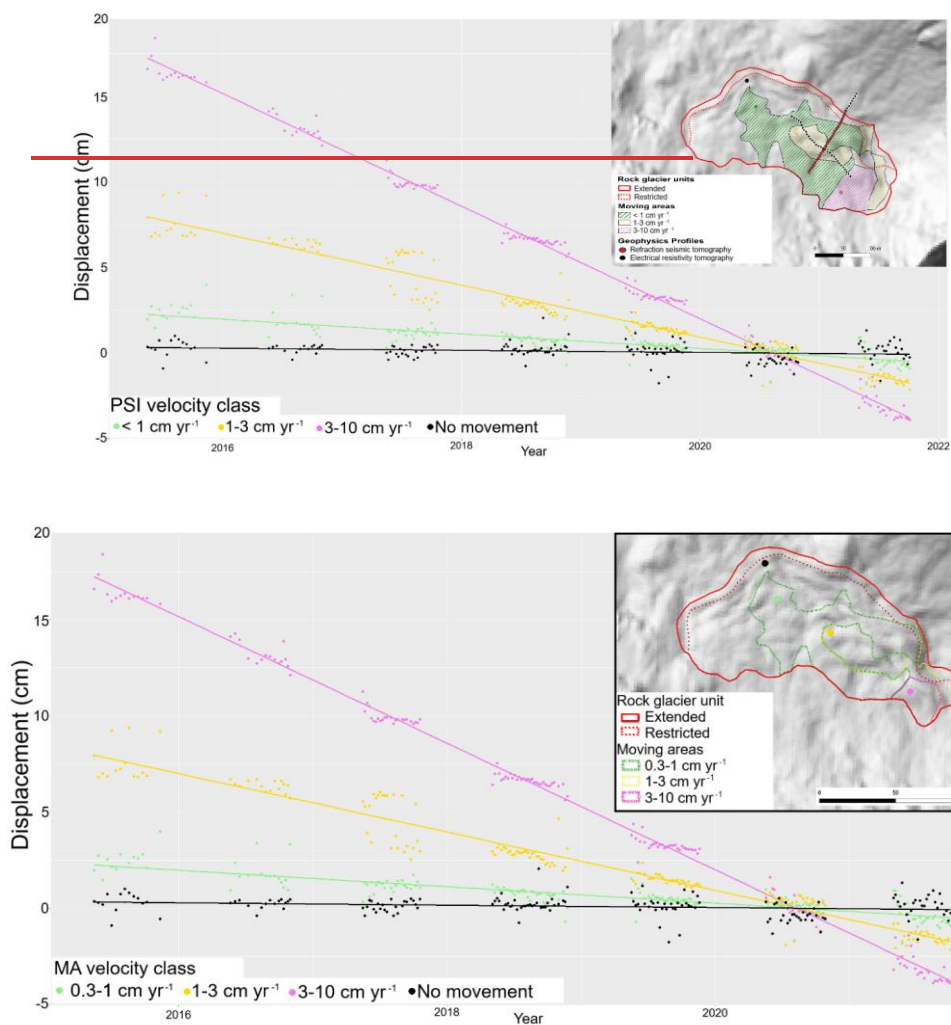
Figure 5: Displacement profiles over a period of 6 years (2015 – 2021) for 4 locations (identified in the location map with dots of corresponding colour) representing each velocity class and one for an area with no movement. The dots show the actual PSI displacement results, while trend lines (linear regressions) indicate long-term motion patterns. The displacement is measured relative to 2021. The downward trend can be interpreted as movement away from the sensor, which in our case represents a combination of

377 **vertical movement and horizontal downslope movement. The gap in point density along the trend line is due to the winter season,**
378 **the measurements being performed in snow free conditions, usually from June to November.**

379 For rock glaciers exhibiting no or minimal movement (< 1 cm yr^{-1}), the RGIK (2023a), recommends assigning a relict activity
380 class. The present analysis shows that only 21 % of the rock glaciers in the Retezat Mountains could be classified as transitional
381 (Fig. 9a), encompassing areas with moving velocities ranging between 1 and 5 cm yr^{-1}. The transitional rock glaciers exhibit
382 a median elevation of 2170 m, surpassing that of the relict ones by 150 m (Fig. 9b). Additionally, the median size of transitional
383 rock glaciers is slightly smaller than that of relict rock glaciers (Fig. 9c).

384

387
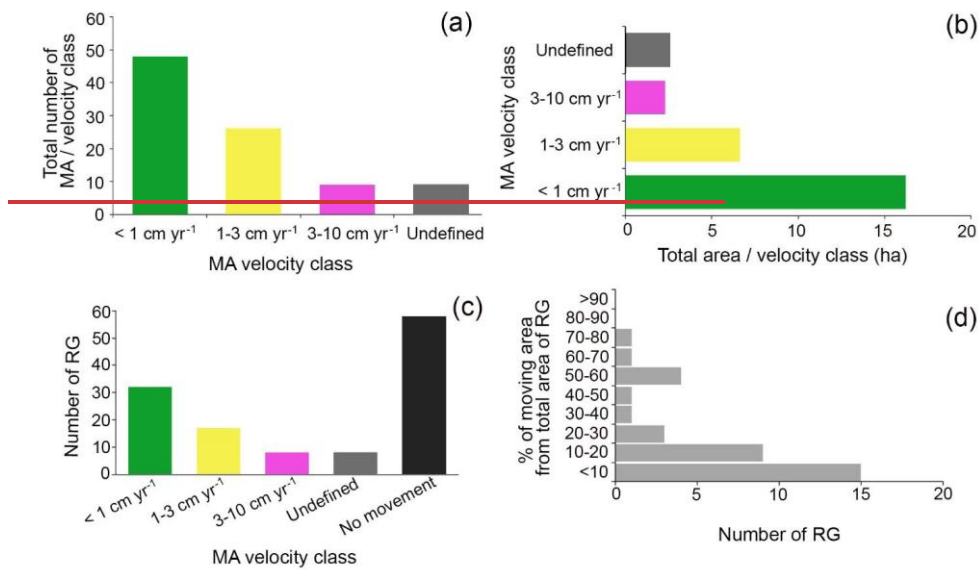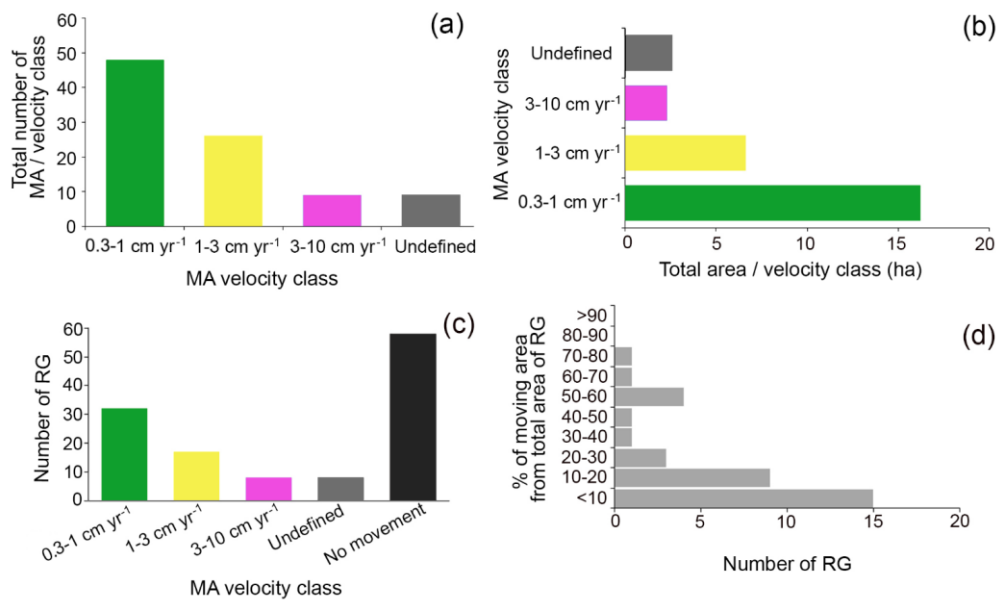
Figure 6: The moving areas classified by velocity classes (a) and their extent (b). The number of rock glaciers containing moving areas and without moving areas (c) and the percentage of the moving area cover within rock glaciers (d).
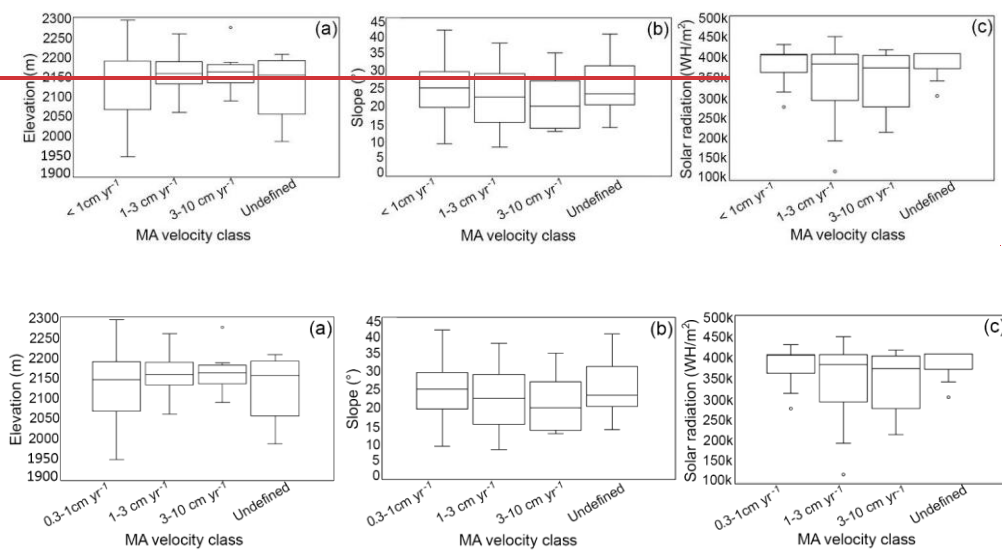
Figure 7: Elevation (a), Slope (b) Potential solar radiation (c) vs MA velocity classes

396
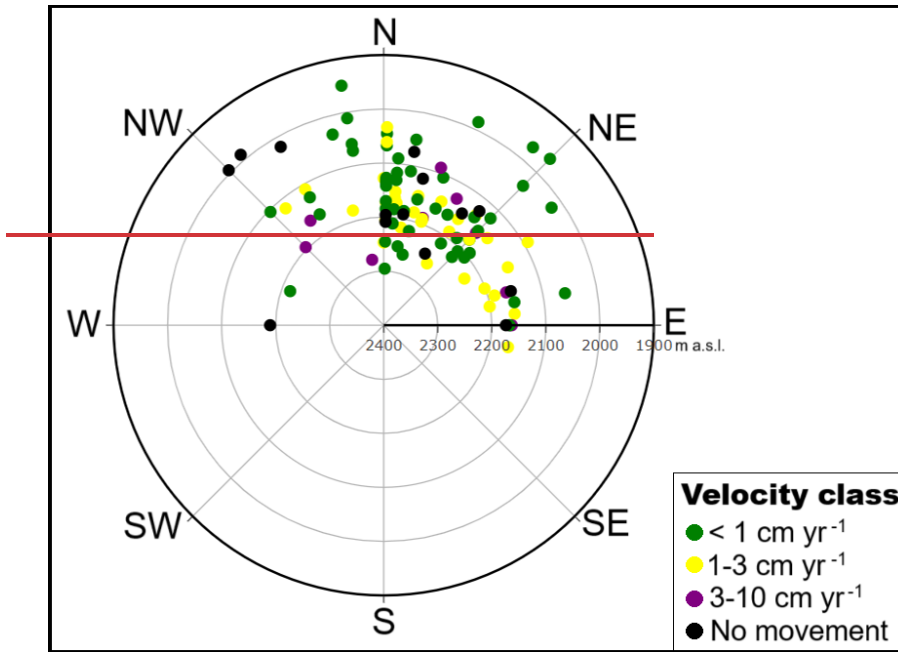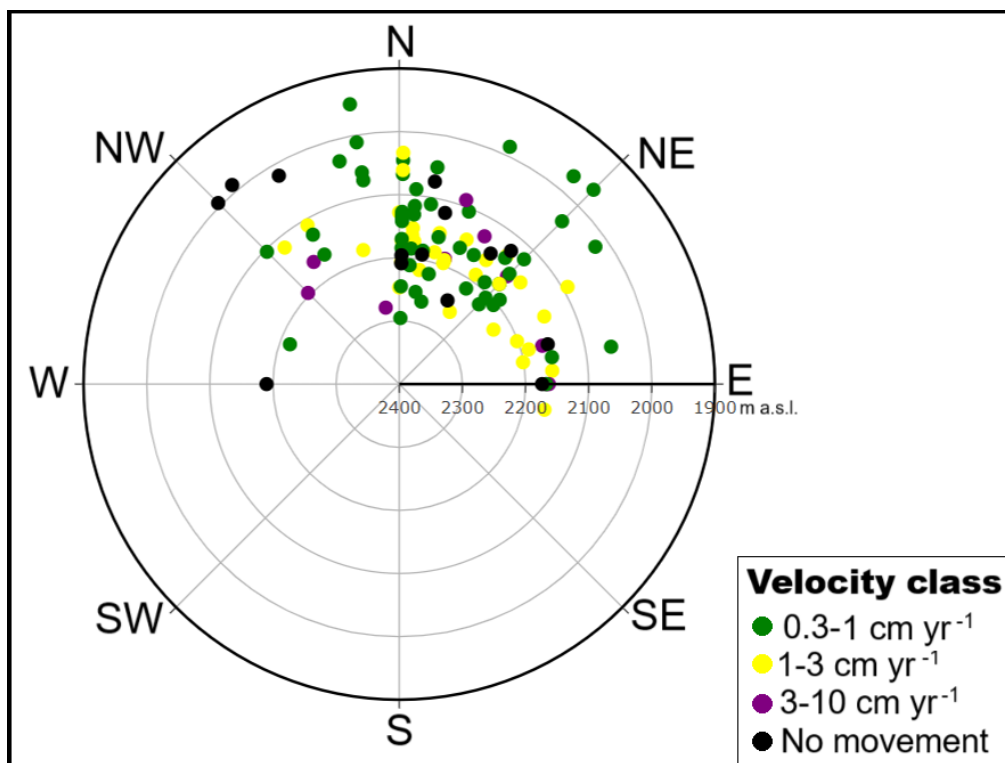
397 **Figure 8: Distribution of moving areas, in the Retezat Mountains, in relation to slope aspect (angular axis) and elevation (radial**
398 **axis).**

399 Figure 10 presents a comparison between ALOS-2 PALSAR-2 interferogram and the Sentinel-1 PSInSAR results at Galeşu

400 (7) site. Although the accuracy of the ALOS-2 PALSAR-2 is lower, both products exhibit similar signals. The main

401 displacement areas are clearly visible and coincide on both maps

402 The comparison between PSI and InSAR performance reveals that, in areas with high spatial variability in displacement, PSI

403 provides more detailed mapping of the ~~monitoring~~ moving areas (MAs), allowing for the differentiation of relatively minor

404 velocity differences. In Fig. 10b, a specific MA is clearly identified and classified as having a velocity of <1 cm yr^{-1}. The same

405 area appears in Fig. 10a, where most of it is also mapped as <1 cm yr^{-1}; however, adjacent zones are classified as 1–3 cm yr^{-1}

406 and 3–10 cm yr^{-1}, indicating a broader range of detected velocities.

407
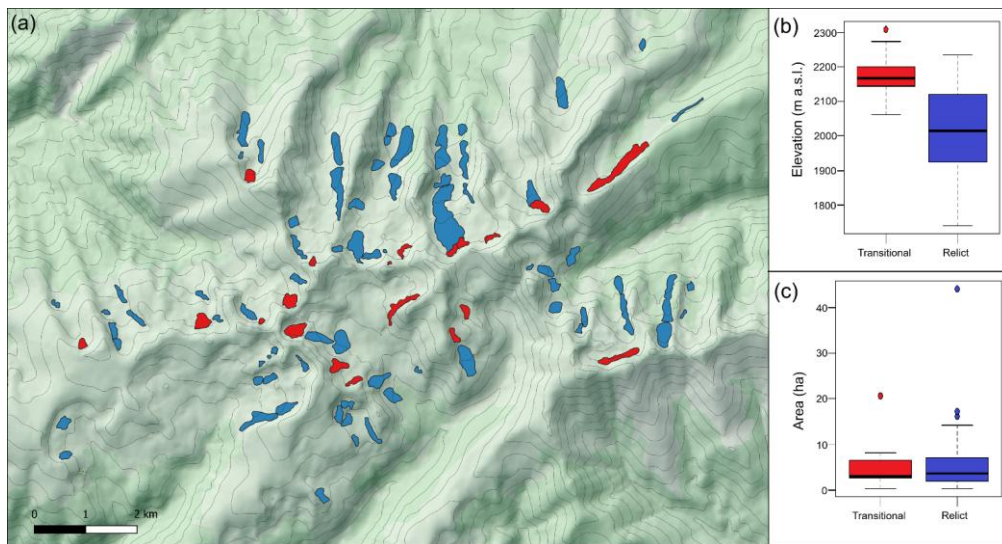
Figure 9: The spatial distribution of transitional and relict rock glaciers in the Retezat Mountains (a) and their median elevation (b) and size (c). Background imagery: Bing Maps © Microsoft, retrieved via QGIS (Version 3.34) using the QuickMapServices.

409

410

411
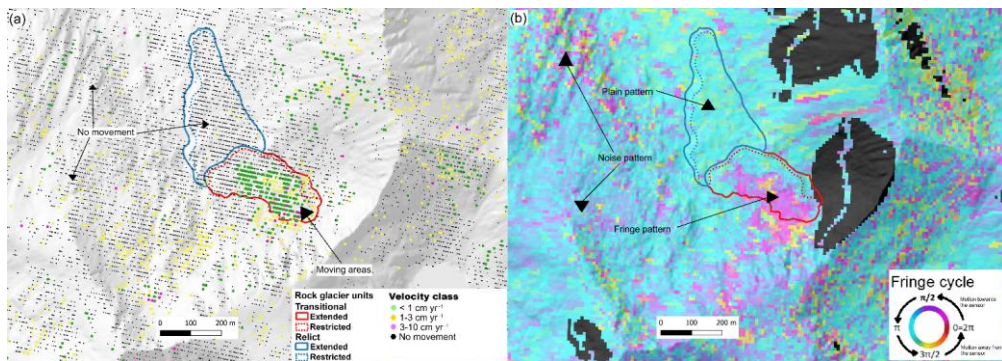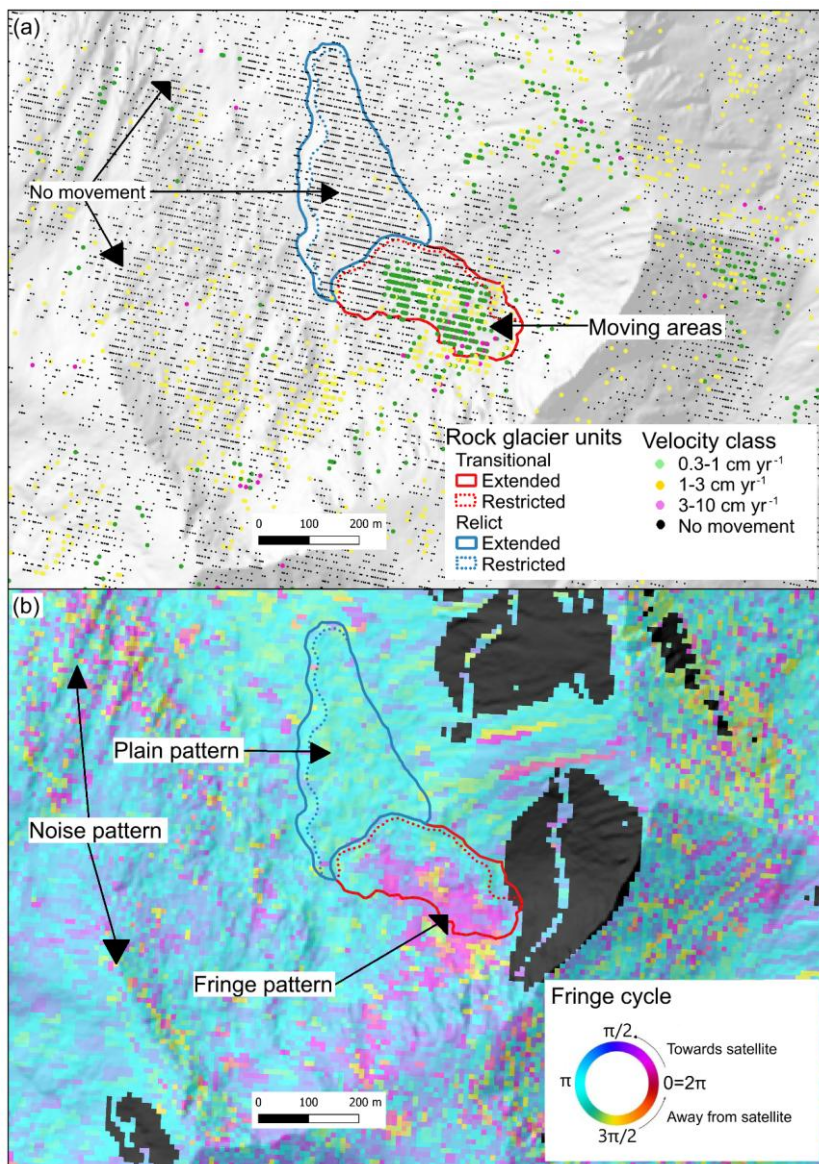
413 **Figure 10: A comparison between multiannual PSINSAR from Sentinel 1 (a) and InSAR from ALOS-2 PALSAR-2 (b). Notice the**
414 **same moving areas inside the RGs, that are revealed by clustered pixels with movement (green, yellow and magenta) from PINSAR**
415 **(a) and the areas with fringe patterns (b). In (b) the shadow areas are masked out and the fringe cycle (bottom right) represents the**
416 **change of colour. The interferogram presented in fig. 10b, over the Galeşu rock glacier unit, ~~Fig. 10b presents the Galeşu RG where~~**
417 **~~in the upper RGU we have one fringe~~ has a long temporal interval, over ~~a~~ five ~~year period (years from~~ September 2014 to October**
418 **2019 ~~.) accounting for a displacement of approximately 0.56 cm/yr. This is in line with the PSI measurements that have the biggest~~**
419 **~~largest MA on the RG to be <1 cm/yr.~~, and it is computed only for the descending path.**

4.2. GNSS measurements

421   The mean velocities measured by dGNSS ranged between 0.4 and 2.8 cm yr^{-1}, with values exceeding 1 cm yr^{-1} for 56 % of the
422   marker points (Fig. 11). On the Judele (8) rock glacier, eight marker points recorded velocities between 1 and 2.6 cm yr^{-1},
423   while nine points showed velocities between 0.4 and 1 cm yr^{-1}. The highest velocities are observed in the central part, gradually
424   decreasing toward the margins. One marker point measured on the front of Judele rock glacier revealed very low rates of
425   displacements (0.4 cm yr^{-1}). Almost all marker points indicate consistent movement toward the front of the rock glacier. Four
426   marker points on the Berbecilor (9) rock glacier revealed velocities between 1 and 2.8 cm yr^{-1} and three between 0.6 and 1 cm
427   yr^{-1}. All the seven marker points indicate consistent movement toward the front. Most marker points with moving velocities
428   between 1 and 2.8 cm yr^{-1} (89 %) were located within MAs categorised under the 1-3 and 3-10 cm yr^{-1} velocity classes by
429   PSInSAR analysis. At Judele, five out of eight dGNSS markers recording velocities between 1 and 2.6 cm yr^{-1}, fall within the
430   1-3 cm yr^{-1} velocity class, whereas at Berbecilor the ratio is two out of four. At both sites, nine marker points with velocities
431   between 0.4 and 1 cm yr^{-1} are located outside any designated MAs, while only three fall~~s~~ within the corresponding velocity
432   class.
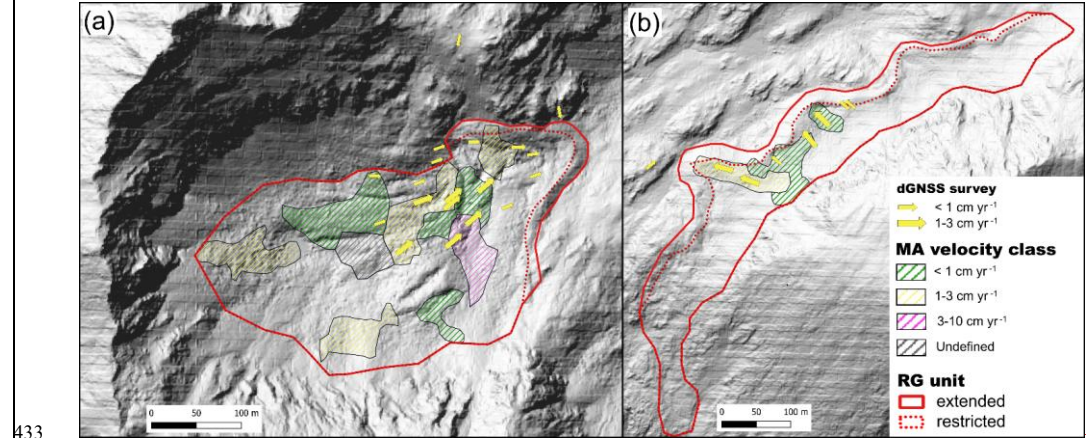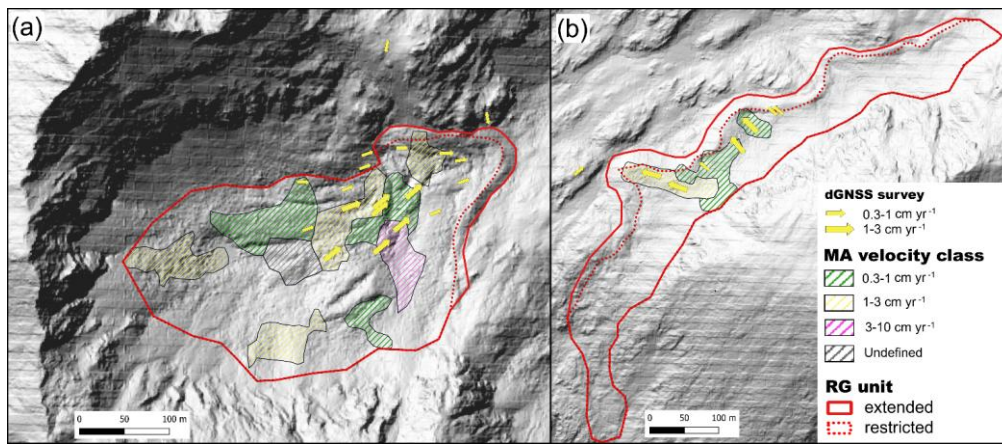
Figure 11: Horizontal displacements derived from GNSS measurements for 2019-2021 at Judele (a) and Berbecilor (b) sites, overlayed on the MAs derived from PSInSAR. Background of both maps: hillshade based on the LAKI II DEM (LAKI II MNT, 2024)

4.3. BTS and ground temperatures

BTS measurements allowed the identification of colder versus warmer ground surface areas in four rock glaciers (Fig. 12). Half of the 140 measured BTS points were measured on Pietrele (3) rock glacier, which has the lowest front altitude and revealed the warmest mean of BTS values (-2.9 ºC). The coldest temperatures at this site occurred in the uppermost part, where most BTS values were below -3 ºC. Several BTS points measured on the talus slope feeding this rock glacier also revealed very low temperatures. In the western part, where a MA in the 0.3-1 cm yr^{-1} velocity class is present, BTS values consistently fell below -5 ºC. At the Galeşu multi-unit rock glacier, the mean BTS was -3.9 ºC, with the coldest values clustered in the southern unit and on the upslope talus. The BTS values within the MAs were all very low, below -5 ºC. In contrast, the northern rock glacier unit, which showed no signs of surface displacement, exhibited a highly heterogeneous distribution of BTS values. Păpușa (6) is the highest rock glacier where BTS measurements were performed and revealed the lowest average of BTS values (-4.1ºC), whereas at Pietricelele (4), the mean BTS was -3.5 ºC. At Păpușa site, a warmer zone occurred in the central part, with three BTS values warmer than -2 ºC; however, all BTS values within the MAs indicated very cold ground conditions Similarly, at Pietricelele, a warmer ground surface area was identified in the central and northeastern parts, while the western and southeastern areas revealed colder temperatures. Snow depth at the probing points ranged from 80 and 260 cm. In all the cases, the calculated median BTS in MAs was lower compared with the median of all BTS values in each site.

458
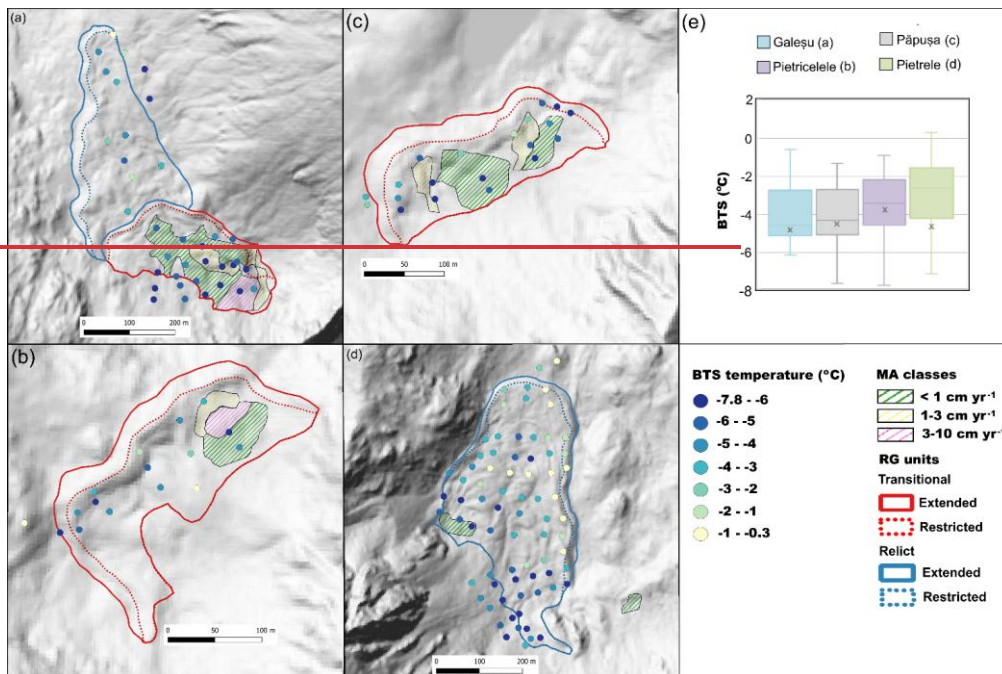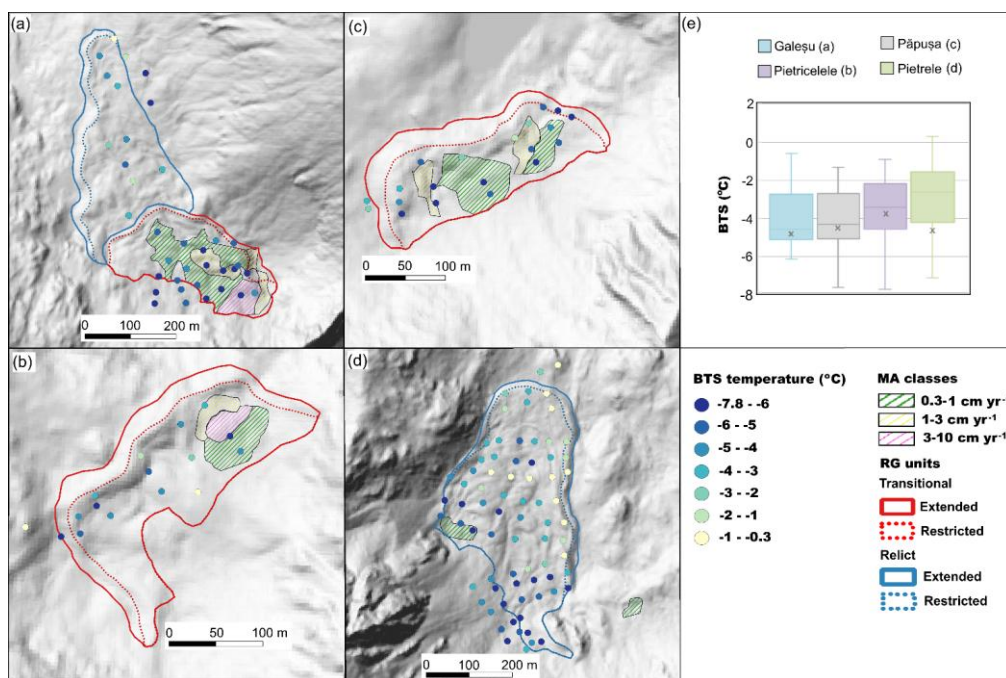
Figure 12: BTS measurements performed in March 2022 on four rock glaciers in the Retezat Mountains: (a) Galeşu, (b) Pietricelele, (c) Păpuşa, (d) Pietrele. (e) Summary box-plot diagram of the BTS measurements, the horizontal line drawn inside denotes the median BTS for each rock glacier, while the x represents the median BTS of the moving areas of each rock glacier). (f) the legend for the maps in (a), (b), (c) and (d).

Between 2013 and 2022, MAGST values at the monitoring sites generally remained below 0 °C, ranging from –2.3 °C to +0.8 °C, with the coldest values at Galeşu and the warmest at Pietrele. ~~In most cases, MAGST values were negative at the monitoring sites from 2013 to 2022, ranging from -2.3 ºC to 0.8 ºC, with the lowest values recorded at Galeşu and the highest at Pietrele~~. To illustrate long-term GST evolution, Figure 13a shows the running annual mean of ground surface temperature. However, subzero MAGST values were recorded only at site Valea Rea (5) in all the years, whereas at Galeşu, all the MAGST values were below 0 ºC except one year (e.g., 2016). All the GST sites revealed negative values for the mean temperature of the entire monitoring interval.

Fig. 13c reveals the mean daily temperature at the GST monitoring sites. The lowest GST values (< -10 ºC) occurred in October-December under snow-free or thin snow cover conditions. This is because the insulating snow cover typically occurs in November/December, whereas the snow disappears in May or June. However, at all the sites, significant ground cooling was observed even during the January-March period, despite snow depths typically being sufficient to insulate the ground from

474 air temperature fluctuations. For example, at Galeşu, almost every winter exhibited notable short-term fluctuations in the GST

475 regime. Similar, through less pronounced, patterns were also observed at Judele (e.g., winters of 2013-2014 and 2017-2018),

476 Pietrele (e.g., 2012-2013, 2013-2014, 2014-2015, 2016-2017 and 2021-2022) and Valea Rea (e.g., 2015-2016 and 2019-2020).

477 In a few instances, inverse thermal relationships between ground surface temperature and air temperature were recorded,

478 confirming the presence of internal ventilation through the coarse debris during winter. These thermal anomalies are likely

479 driven by advective heat fluxes that remain active beneath thick snow cover and likely contribute to the cold MAGST observed

480 in the rock glaciers. Usually, during March, ground surface temperatures are relatively stable and are mainly driven by

481 conductive processes. In almost all cases, the corresponding WEqT were below -2 ºC, indicating possible or probable

482 permafrost occurrence (Fig. 13b). WEqT values higher than -2 ºC occurred only at Pietrele in late winter 2013 and 2014. At

483 Valea Rea and Judele, most WEqT values were between -2 and -3 ºC, whereas at Galeşu, the late winter temperatures were

484 considerably lower.
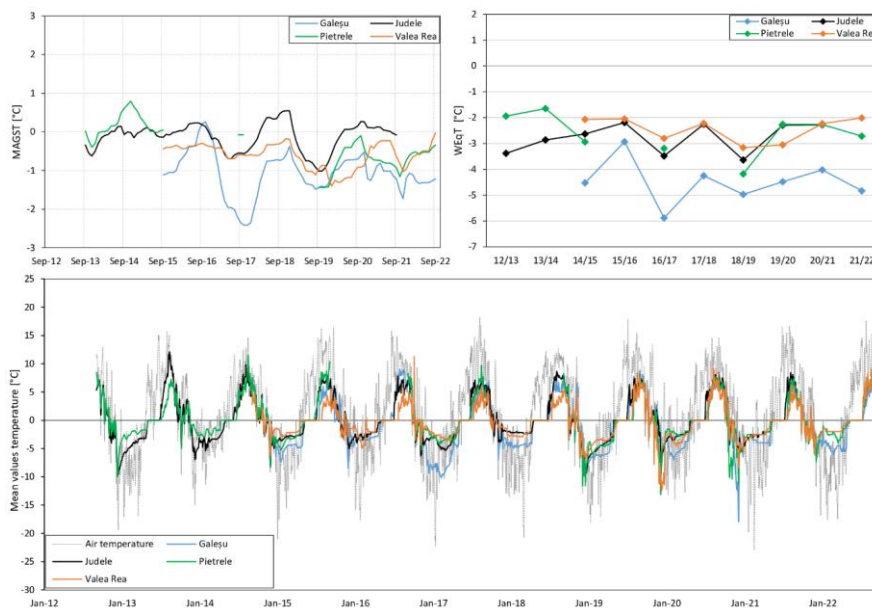
486 **Figure 13: (a) Running 12-month average of mean annual ground surface temperature, (b) Winter Equilibrium Temperature**
487 **(WEqT) and (c) Running 12 months average of Ground Surface Temperature (GST) for the period 2012/2013 to 2021/2022 at four**
488 **sites in the Retezat Mountains and air temperature at Ţarcu meteorological station (2180 m).**

4.4. Geophysics results

The results of the geophysical surveys at Galeşu rock glacier are shown in Figure 14 for the two crossing ERT profiles P1 and P2 (Fig. 14a, b), as well as the RST and PJI results available for profile P1 (Fig. 14c, d). Both ERT tomograms reveal an up to 5 m thick layer characterised by high resistivities (> 200 kΩm) representing the dry and coarse-blocky surface layer. Patchy occurrences with similarly high resistivities are observed in 5-20 m depth in both profiles, which could indicate remnants of former ice-rich permafrost within the rock glacier (labelled with `ice?` in Fig. 14). Below, a more homogeneous layer of resistivities around 10 – 30 kΩm may indicate the rock glacier base (bedrock) in the southwestern part of profile P1, however, the resistivity values do not exclude the possibility of frozen conditions and the interpretations of this zone remains ambiguous. The landform's overall thickness is estimated at < 20 – 30 m and potentially < 15 m in the southwestern part of profile P1. The eastern part of profile P1 (x < 50 m in Fig. 14b) is located outside the rock glacier and traverses into a partially vegetated talus slope. Here, the surface layer exhibits lower resistivities (< 100 kΩm, probably representing smaller block size and organic material), and the underlying resistive layer (100-200 kΩm) has a thickness of about 10 m and a more homogeneous appearance than that of the rock glacier. Both the morphology and the resistivity values point to a potentially frozen ventilated talus slope, but this is not a focus of this study and will not further be explored.

504
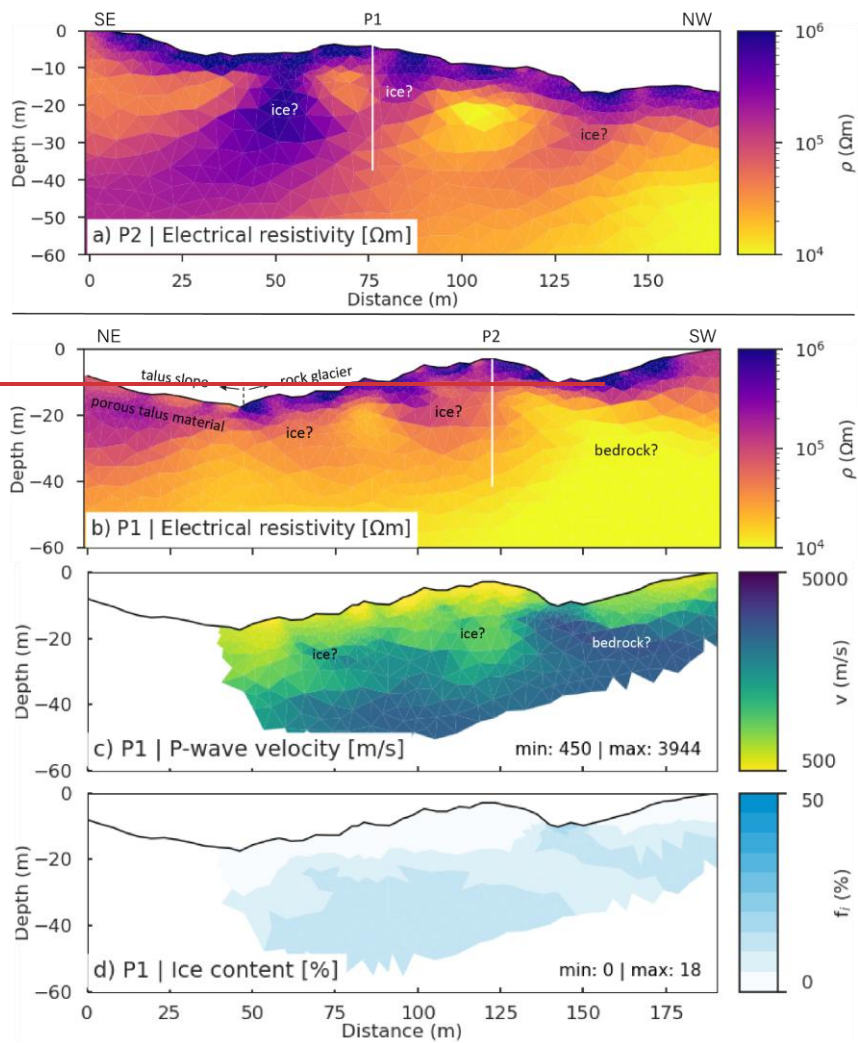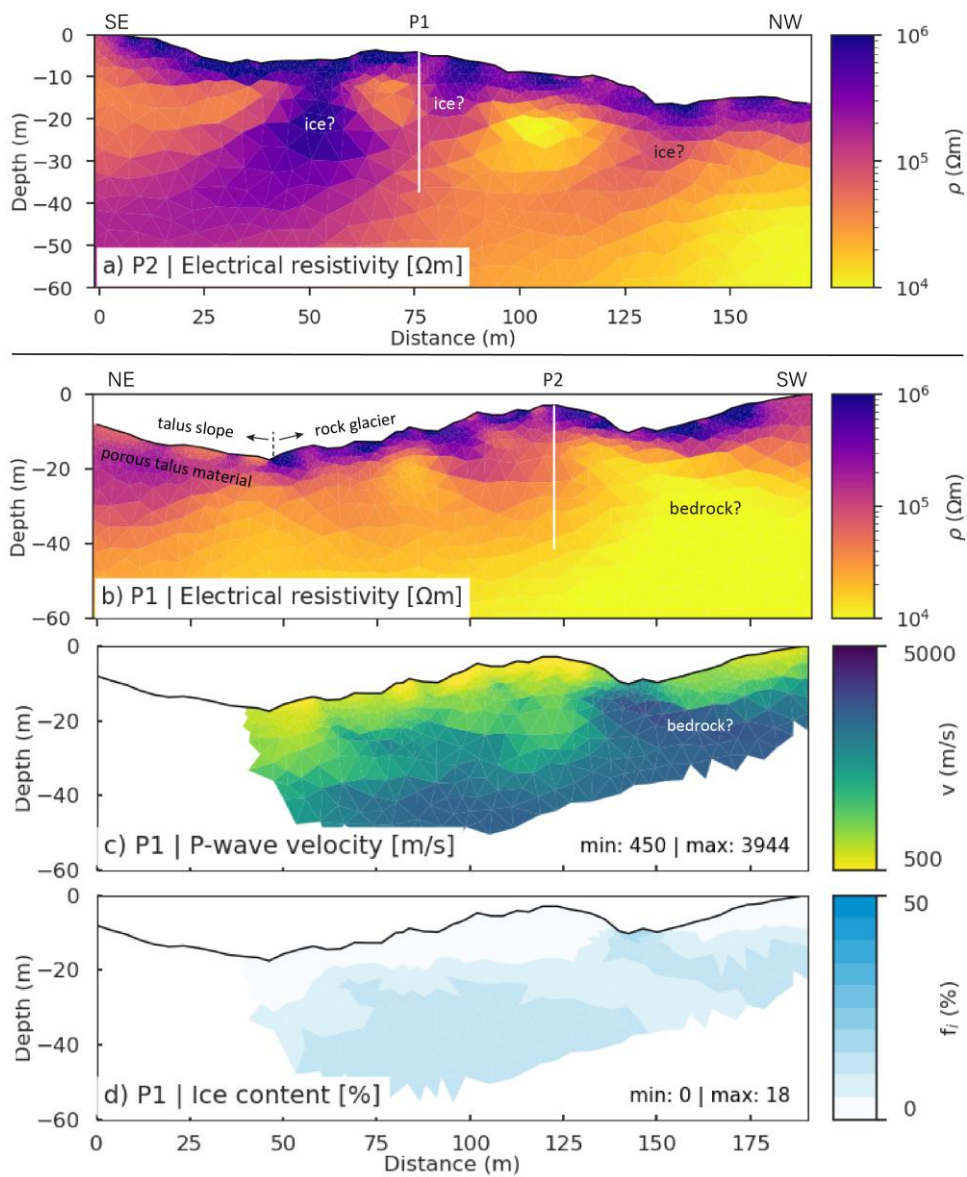
Figure 14: a) and b) ERT profiles P2 and P1 (see Fig. 1c for location), c) RST profile, and d) modelled ground ice content based on the PJI.

The seismic profile P1 (Fig. 14c) only covers the rock glacier part of the ERT profile P1 and shows a 5-10 m thick upper layer with P-wave velocities < 1500 m s-1, indicating highly porous blocky material. The velocities are increasing with depth, reaching 4000 m s-1 at about 20-25 m depth in the central part of the rock glacier and at shallower depths (~ 15 m) in the last 50 m of the profile. According to the seismic data, ice-rich permafrost would be possible in large parts of the tomogram. However, in combination with the ERT data, ice-rich conditions seem only plausible in those parts of the tomogram that coincide with elevated resistivities. Alternatively, the zones with lower resistivities could also indicate zones with increased conductivity due to ongoing ice melt, the interpretation therefore remains ambiguous. The seismic data further indicate relatively porous material rather than firm bedrock and point to an overall larger thickness of the rock glacier than indicated by the ERT profile.

The result of the PJI modelling (Fig. 14d) reveals a generally very low ground ice content in the upper sector of the Galeşu rock glacier, with maximum values of 18 %. The highest ice contents coincide with zones with highest seismic velocity, partly contradicting the individual interpretation (bedrock). This can be due to the known rock-ice ambiguity of the current PJI formulation, as the rock and ice content are only directly constrained through the petrophysical equation of the seismic velocity. As a consequence, the correct differentiation between rock and ice is problematic in some cases (see Mollaret et al., 2020 for details). The generally low ice contents modelled through the PJI therefore mainly confirm that a potential former massive ice core is not detectable anymore and point to an advanced state of degradation of this rock glacier. However, these results do not exclude the possibility of more confined ice-saturated or even supersaturated layers (as expected based on the analysis of InSAR data in section). Due to the limited resolution capacity of the geophysical profiles with 4 m sensor spacing thin ice-rich or ice-supersaturated layers may not be resolvable as such, but - depending on their depth and extent - with strongly reduced spatial gradients of the ice content (as well as resistivity or velocity contrast in the individual tomograms). The relatively homogeneous ice content distribution modelled from the PJI may therefore not only reflect the rock-ice ambiguity mentioned above, but also this limitation to resolve small-scale structures.

5. Discussion

5.1. Assessing the velocity of rock glaciers in marginal periglacial environments

In marginal periglacial regions rock glaciers exhibit a minimal rate of motion (a few cm yr^{-1}) (Necsoiu et al., 2016) and evaluating their velocity can pose occasional challenges. Hence, the compilation of MAs inventory might be affected by limitations associated with radar interferometry (Bertone et al., 2022).

The PSInSAR measurements were provided in the SAR LOS direction, representing a 1-D rather than a 3-D measurement, capturing only a single component of motion. Due to the particular steep topography of the study area, it can be assumed that

538 the movement direction of the actual motion is oriented along the mountain slope. Although PSInSAR does not produce the
539 exact 3-D velocity vectors, this work was helpful in detecting areas of motion and refining the rock glaciers inventory.

540 Slow-moving areas (i.e., 0.3-1 cm yr^{-1}; 1-3 cm yr^{-1}) are prevalent in this region, where only 10% of the MAs are characterised
541 by velocities exceeding 3 cm yr^{-1}. The latter tend to occupy higher elevations and receive less solar radiation than slower ones.
542 Overall, the median size of the MAs from Retezat Mountains is slightly smaller than other periglacial environments (Bertone
543 et al., 2022). The median size of the MAs, showing minimal variation across velocity classes, exhibits a slight peak among
544 those moving at < 1 cm yr^{-1} (0.33 ha). The median size of MA velocity classes of 1-3 cm yr^{-1} and 3-10 cm yr^{-1} is 0.3 ha, roughly
545 one-third smaller than those reported in Southern Tyrol (Bertone et al., 2024).

546 The examination of displacement measurements through the differential GNSS technique unveiled similarly very slow
547 movements at specific points (ranging from a few millimetres to 2.8 cm yr^{-1}). A comparison between the GNSS survey and
548 PSInSAR results revealed that there was not a very good correspondence between these outcomes. The discrepancy may be
549 due to the difficulty both methods have in accurately detecting such slow movement. Additionally, differences between the
550 velocity datasets may result from the distinct time intervals used for analysis - 2015-2021 for PSInSAR and 2019-2021 for
551 dGNSS. However, most GNSS survey markers that exhibited horizontal displacements exceeding 1 cm yr^{-1} were still located
552 within the MAs. In terms of flow direction, the majority of these markers indicated consistent movement toward the fronts of
553 Judele and Berbecilor rock glaciers, behavior characteristic of permafrost creep.

554 The PSInSAR analysis enriches the existing rock glacier inventory with information about the activity status of rock glaciers
555 in the Retezat Mountains. A previous study classified 30 rock glaciers in the study area as intact based on geomorphological
556 and ecological criteria (Onaca et al., 2017b). Radar interferometry revealed that 20 rock glaciers exhibit surface displacements
557 exceeding 1 cm yr^{-1}. In contrast, 15 rock glaciers showed minimal displacements (0.3 – 1 cm yr^{-1}). Of these, eight were
558 previously classified as intact, while the remaining seven were categorised as relict. Four rock glaciers, previously labelled as
559 geomorphologically relict, show surface displacements exceeding 1 cm yr^{-1} and were categorised as transitional in our study.
560 Unlike other regions (e.g., Central Italian Alps, Eastern European Alps, Himalaya) where there is a considerable elevation
561 difference between active/intact and relict rock glaciers (Kellerer-Pirklbauer et al., 2012; Scotti et al., 2013), the Retezat
562 Mountains exhibit a significantly smaller separation.

5.2. Permafrost occurrence revealed by geophysical and temperature measurements

564 The geophysical investigations revealed a frozen layer with overall low ice contents beneath a substantial active layer of
565 approximately 5 m thickness. Similar results have been reported in other marginal periglacial environments (i.e., Făgăraș
566 Mountains, Pirin Mountains, Italian Carnic Alps) where thick active layers indicate even greater thickness (Onaca et al., 2013;
567 Colucci et al., 2019; Onaca et al., 2020). Due to the rock glacier's very dry and extremely coarse blocky surface, the ERT data
568 only have limited quality which is also reflected by the high resistivities of > 200 kΩm on the rock glacier surface. However,
569 we still assume that the overall resistivity pattern indicates the main structures and is representative for the site, whereas small-
570 scale anomalies present in the tomograms as well as absolute resistivity values, should be interpreted with care.

571 The BTS measurements revealed very cold surface temperatures (< -4 ºC) across large portions of the rock glaciers, with
572 particularly low values observed within MAs, in the upper sections of the rock glaciers, and along the upper talus slopes.
573 However, not all cold areas exhibited detectable movement in the PSInSAR results. Conversely, considerably warmer ground
574 surface temperatures (-2 – -0.3 ºC) were also recorded in various parts of the rock glaciers, supporting the presence of internal
575 ventilation. The GST results suggest favourable conditions for permafrost existence, but more notably highlight significant
576 ground cooling episodes during the winter, likely driven by air advection. Similar results have been reported for Judele,
577 Pietrele, Valea Rea, Galeşu and Pietricelele rock glaciers in previous studies (Vespremeanu-Stroe et al., 2012; Onaca et al.,
578 2015). Except for Pietrele, the other data-logger sites (Galeşu, Judele and Valea Rea) are located in areas with displacement
579 velocities exceeding 1 cm yr^{-1}. However, at Pietrele, despite the prevalence of low BTS values, almost no displacement was
580 observed, except in the western part, where minor displacements (0.3 – 1 cm yr^{-1}) were detected. The Pietrele rock glacier is
581 oriented along a south-north direction and the LOS orientation tends to underestimate displacements on north facing slopes
582 (Liu et al., 2013). The lack of significant displacement in this rock glacier between 2014 and 2021 does not necessarily indicate
583 complete ice melt, but likely suggests ~~negligible~~ an insufficient ice content for permafrost creep to occur.

5.3. Rock glaciers behaviour in marginal periglacial environment

585 The rock glaciers in the Southern Carpathians generally move at slower rates than those in other mid-latitude high mountains,
586 where rock glaciers' velocities range from a few centimetres to a few meters per year. But rock glaciers experiencing very low
587 movement velocities were also documented in different periglacial regions (e.g., Pyrenees, Rocky Mountains, northern
588 Norway, Southern Alps of New Zealand, etc.) (Serrano et al., 2010; Brencher et al., 2021; Rouyet et al., 2021; Bertone et al.,
589 2022; Lambiel et al., 2023). In the Retezat Mountains, only 21 % of the inventoried rock glaciers display motion, whereas the
590 rest are considered relict. Similar to the Uinta Mountains (Brencher et al., 2021), in most cases, only a relatively reduced
591 portion of the rock glacier exhibits movements. An illustrative case in this regard is the Galeşu multi-unit rock glacier,
592 displaying movement solely in its uppermost unit, where a younger lobe overlies the main body of the rock glacier. Similar
593 younger lobes were identified in other valleys (e.g., Valea Rea, Pietrele) representing distinct phases of rock glaciers activity,
594 as observed in many other periglacial regions of Europe (e.g. Iceland, European Alps, Cantabrian Mountains, Pyrenees etc.)
595 (Farbrot et al., 2007; Kellerer-Pirklbauer et al., 2008; Steinemann et al., 2020; Amschwand et al., 2021; Oliva et al., 2021;
596 Santos-González et al., 2022).
597 Additionally, the PSInSAR analysis revealed that, in many instances, the fronts of the rock glaciers in the Retezat Mountains
598 remain stable. Notable examples of stable fronts include Judele (Fig. 11a), Berbecilor (Fig. 11b), Galeşu (Fig. 12a), Păpuşa
599 (Fig. 12c) and Pietricelele (Fig. 12b). Field observations also confirmed that despite steep and sometimes unvegetated slopes,
600 the rock glacier fronts display no recent activity, and no ploughed grass occurs at their snouts. This type of rock glacier, called
601 climatically inactive (Barsch, 1996), is also distinguished by a substantial unfrozen mantle and a low ice content (Onaca et al.,
602 2013).

603 The geophysical measurements performed in this study indicated the very low ice content in the Galeșu rock glacier,
604 insufficient to support permafrost creep. For permafrost creep to occur, frozen conditions must extend to a depth of at least 10-
605 25 m (Cicoira et al., 2021), which does not appear to be the case at Galeșu. Surface displacements at this site are more likely
606 the result of ice-melt-induced subsidence, solifluction, or the tilting and sliding of blocks within the active layer. In contrast,
607 the flow direction of dGNSS markers at Judele and Berbecilor showed consistent movement patterns, which are not typical of
608 ice-melt subsidence or any other active-layer processes. Additional geophysical and dGNSS measurements are needed to better
609 distinguish between these mechanisms in marginal periglacial environments.

610 Various studies suggest that the volumetric ice content within active rock glaciers typically falls within the range of 40 % to
611 60 % (Barsch, 1996; Hausmann et al., 2007; Rangecroft et al., 2015). Conversely, for rock glaciers tending towards inactivity,
612 Wagner et al. (2021) propose average ice content as low as 20 %. These estimates are commonly used to assess the water
613 volume equivalent of ice content stored in rock glaciers (Wagner et al., 2021; Pandey et al., 2024). However, the geophysical
614 investigations presented in this paper reveal even lower values for the volumetric ice content of the Galeșu rock glacier. This
615 finding suggests that the ice content in transitional rock glaciers may be considerably lower than expected, emphasising caution
616 when calculating water volume equivalent on a broad scale.

617 Considering the current MAGST of approximately -0.5 ºC and assuming a climatic warming of about +1.5 ºC since the late
618 19th century (Allen et al., 2018), it is likely that these rock glaciers had a MAGST around -2 ºC during the pre-industrial period.
619 At such low temperatures, widespread permafrost conditions would have been expected, and the presence of deep permafrost
620 cannot be ruled out. However, accelerated warming in recent decades has resulted in permafrost warming, particularly in ice-
621 poor bedrock, at rates comparable to the increase in air temperature (Noetzli et al., 2024). BTS measurements and GST patterns
622 observed during winter suggest ongoing convective and advective air flow processes that maintain cold ground conditions and
623 support the persistence of ice non-saturated permafrost in the Retezat Mountains.

624 The results presented in this study align with the coarse-rock glacier hypothesis (Onaca et al., 2015; Popescu et al., 2017),
625 which suggests that permafrost occurrence in the Carpathian Mountains is patchy and limited to sites above 2100 m with low
626 solar radiation. In these locations, very coarse rock glaciers, hosting numerous large boulders, facilitate strong cooling through
627 internal ventilation (e.g., advection and convection) (Wicky and Hauck, 2017; Amschwand et al., 2024) and air stratification
628 (low conductivity) during summer or under thick snow cover.

629 **6. Conclusions**

630 This study leads to the following main conclusions:

631 - The majority of rock glaciers in the marginal periglacial environment of the Retezat Mountains are classified as relict,
632 with only 21% categorized as transitional. The median elevation of transitional rock glaciers is 150 m higher than that of relict
633 rock glaciers and their median size is slightly smaller. The PSInSAR methodology enabled the identification of new rock
634 glaciers displaying movements, which were initially classified as relict features.

635   -   A total of 92 moving areas were delineated within the rock glaciers of the Retezat Mountains, predominantly falling
636 within the slow-velocity classes (0.3 – 1 cm yr^{-1} and 1-3 cm yr^{-1}). Moving areas exhibiting velocities between 1 and 5 cm yr^{-1}
637 are typically located above 2100 m in regions with minimal solar radiation income. Higher movement rates are observed in
638 the upper, younger lobes compared to the well-developed lower parts.

639   -   Long-term ground temperature monitoring from 2012 to 2022 revealed low MAGST values at the observation sites,
640 ranging from -2.3 ºC to 0.8 ºC. Internal ventilation processes (e.g., advection) occurring throughout the winter significantly
641 contribute to surface cooling and appear to sustain permafrost conditions in coarse debris above 2100 m. This is further
642 supported by BTS measurements, which indicate very cold ground temperatures beneath a thick late-winter snow cover.

643   -   Geophysical measurements conducted on an intact rock-glacier revealed notably low ice content (with maximum
644 values of 18%) in its uppermost section. At this site, surface displacements are most likely driven by processes such as ice-
645 melt-induced subsidence, solifluction or blocks sliding. In contrast, the consistent flow of dGNSS markers towards the fronts
646 of the Judele and Berbecilor rock glaciers points to permafrost creep.

647 Our findings highlight the value of combining Sentinel-1 SAR data with extensive field investigation (such as DGPS,
648 geophysical and thermal methods) and where possible, with other remote sensing data (like ALOS-2 PALSAR-2), particularly
649 in regions with slow-moving rock glaciers. This approach could serve as a benchmark for similar studies in marginal periglacial
650 environments.

651 **Code/Data availability**

652 The deformation data, obtained using PSI, and the temperature data, obtained using GST data loggers and BTS are freely
653 available as a Zendo repository, at https://zenodo.org/records/14544941, DOI: 10.5281/zenodo.14544940
654 For further questions about data processing readers are encouraged to contact the authors.

655 **Author Contribution**

656 The study was conceptualized and managed by AO and FS. AO led the manuscript writing, with contributions from VP, CH,
657 PU, TS and FS. VP, TS, DT, DB and FS contributed to the PSInSAR analysis. FA and IL produced the inventory of moving
658 areas and performed the statistical analysis related to rock glaciers. AO, OB, RP, MV, IL and AVS contributed to the analysis
659 of thermal measurements. CH, BE, SF, RP and AO were involved in conducting and analysing the geophysical measurements.
660 AH and AO provided the GNSS measurements. All authors provided feedback on the final version of the paper.

661 **Competing interests**

662 The authors declare that they have no conflict of interest.

Acknowledgements

This research was funded by the ESA Permafrost_CCI project (grant number 4000123681/18/I-NB), EEA Norway Grants 2014–2021, under project code RO-NO-2019-0415 / contract no. 30⁄2020 and PNRR-III-C9 2022 - I8, CF 253/29.11.2022, 760055/23.05.2023. We would also like to thank Sabina Calisevici, Adrian C. Ardelean, Patrick Chiroiu, Trond Eiken, Romolus Mălăieștean, Ilie Adrian and Fabian Timofte for support in the fieldwork.

References

Allen, M. R., Dube, O. P., Solecki, W., Aragón-Durand, F., Cramer, W., Humphreys, S., Kainuma, M., Kala, J., Mahowald, N., Mulugetta, Y., Perez, R., Wairiu, M., and Zickfeld, K.: Framing and Context, In: Global Warming of 1.5 °C, In: An IPCC Special Report on the impacts of global warming of 1.5 °C above pre-industrial levels and related global greenhouse gas emission pathways, in the context of strengthening the global response to the threat of climate change, edited by: Masson-Delmotte, V., Zhai, P., Pörtner, H.-O., Roberts, D., Skea, J., Shukla, P. R., Pirani, A., Moufouma-Okia, W., Péan, C., Pidcock, R., Connors, S., Matthews, J. B. R., Chen, Y., Zhou, X., Gomis, M. I., Lonnoy, E., Maycock, T., Tignor, M., and Waterfield, T., Cambridge University Press, Cambridge, UK and New York, NY, USA, pp. 49–92, https://doi.org/10.1017/9781009157940.003, 2018.

Amschwand, D., Ivy-Ochs, S., Frehner, M., Steinemann, O., Christl, M., and Vockenhuber, C.: Deciphering the evolution of the Bleis Marscha rock glacier (Val d'Err, eastern Switzerland) with cosmogenic nuclide exposure dating, aerial image correlation, and finite element modeling, The Cryosphere, 15, 2057–2081, https://doi.org/10.5194/tc-15-2057-2021, 2021.

Amschwand, D., Scherler, M., Hoelzle, M., Krummenacher, B., Haberkorn, A., Kienholz, C., and Gubler, H.: Surface heat fluxes at coarse blocky Murtèl rock glacier (Engadine, eastern Swiss Alps), The Cryosphere, 18, 2103-2139 https://doi.org/10.5194/tc-18-2103-2024, 2024.

Archie, G. E.: The electrical resitivity log as an aid in determining some reservoir characteristics, Petroleum Transactions of American Institute of Mining and Metallurgical Engineers (AIME), 146, 54–62, https://doi.org/10.2118/942054-G, 1942.

Barboux, C., Delaloye, R., and Lambiel, C.: Inventorying slope movements in an Alpine environment using DInSAR, Earth Surf. Processes, 39, 2087–2099, https://doi.org/10.1002/esp.3603, 2014.

Barsch, D.: Rockglaciers: Indicators for the Present and Former Geoecology in High Mountain Environments, Springer, Berlin, 331 pp, ISBN 3-540-60742-0, 1996.

Bernhard, L., Sutter, F., Haeberli, W., Keller, F.: Processes of snow/permafrost-interaction at a high-mountain site, Murtél/Corvatsch, Easterns Swiss Alps, in 7th International Conference on Permafrost, Yellowknife, Canada, Collection Nordicana, vol. 57, 35-41, 1998.

Bertone, A., Barboux, C., Bodin, X., Bolch, T., Brardinoni, F., Caduff, R., Christiansen, H. H., Darrow, M. M., Delaloye, R., Etzelmüller, B., Humlum, O., Lambiel, C., Lilleøren, K. S., Mair, V., Pellegrinon, G., Rouyet, L., Ruiz, L., and Strozzi, T.:

Incorporating InSAR kinematics into rock glacier inventories: insights from 11 regions worldwide, The Cryosphere 16, 2769–2792, https://doi.org/10.5194/tc-16-2769-2022, 2022.

Bertone, A., Jones, N., Mair, V., Scotti, R., Strozzi, T., and Brardinoni, F.: A climate-driven, altitudinal transition in rock glacier dynamics detected through integration of geomorphological mapping and synthetic aperture radar interferometry (InSAR)-based kinematics, The Cryosphere, 18, 2335–2356, https://doi.org/10.5194/tc-18-2335-2024, 2024.

Berzescu, O., Ardelean, F., Urdea, P., Ioniță, A., and Onaca, A.: Thermal Regime Characteristics of Alpine Springs in the Marginal Periglacial Environment of the Southern Carpathians, Sustainability, 17(9), 4182, https://doi.org/10.3390/su17094182, 2025. ~~Berzescu, O., Ardelean, F., Urdea, P., Ioniță, A., and Onaca, A.: Thermal regime characteristics of alpine springs in the marginal periglacial environment of the Southern Carpathians, Sustainability, in press, 2025.~~

Brencher, G., Handwerger, A.L., and Munroe, J.S.: InSAR-based characterization of rock glacier movement in the Uinta Mountains, Utah, USA, The Cryosphere, 15, 4823-4844, https://doi.org/10.5194/tc-15-4823-2021, 2021.

Cicoira, A., Beutel, J., Faillettaz, J., and Vieli, A.: Water controls the seasonal rhythm of rock glacier flow, Earth Planet. Sc. Lett., 528, 115844, https://doi.org/10.1016/j.epsl.2019.115844, 2019.

Cicoira, A., Marcer, M., Gärtner-Roer, I., Bodin, X., Arenson, L. U., Vieli, A.: A general theory of rock glacier creep based on in-situ and remote sensing observations, Permafrost Periglac., 32, 139-153, https://doi.org/10.1002/ppp.2090, 2021.

Colucci, R.R., Forte, E., Žebre, M., Maset, E., Zanettini, C., and Guglielmin, M.: Is that a relict rock glacier?, Geomorphology, 330, 177–189, https://doi.org/10.1016/j.geomorph.2019.02.002, 2019.

Crosetto, M., Monserrat, O., Cuevas-González, M., Devanthéry, N., and Crippa, B.: Persistent Scatterer Interferometry: A review. ISPRS J. Photogramm., 115, 78–89, http://dx.doi.org/10.1016/j.isprsjprs.2015.10.011, 2016.

Delaloye, R., and Lambiel, C.: Evidence of winter ascending air circulation throughout talus slopes and rock glaciers situated in the lower belt of alpine discontinuous permafrost (Swiss Alps), Nor. Geogr. Tidsskr., 59, 194-203, https://doi.org/10.1080/00291950510020673, 2005.

Delaloye, R., Morard, S., Barboux, C., Abbet, D., Gruber, V., Riedo, M., and Gachet, S.: Rapidly moving rock glaciers in Mattertal. In: *Graf, C.* (ed.) Mattertal – ein Tal in Bewegung. Publikation zur Jahrestagung der Schweizerischen Geomorphologischen Gesellschaft 29. Juni – 1. Juli 2011, St. Niklaus. Birmensdorf, Eidg. Forschungsanstalt WSL. 21-30, 2013.Eriksen, H. Ø., Rouyet, L., Lauknes, T. R., Berthling, I., Isaksen, K., Hindberg, H., Larsen, Y., and Corner, G. D.: Recent Acceleration of a Rock Glacier Complex, Ádjet, Norway, Documented by 62 Years of Remote Sensing Observations, Geophys. Res. Lett., 45, 8314–8323, https://doi.org/10.1029/2018GL077605, 2018.

European Environment Agency (EEA): EGMS Algorithm Theoretical Basis Document (ATBD), Copernicus Land Monitoring Service, (https://land.copernicus.eu/en/technical-library/egms-algorithm-theoretical-basis-document/@@download/file), accessed 18 April 2025.

Farbrot, H., Etzelmüller, B., Guðmundsson, Á., Humlum, O., Kellerer-Pirklbauer, A., Eiken, T., and Wangensteen, B.: Rock glaciers and permafrost in Tröllaskagi, Northern Iceland, Z. Geomorphol., 51, 1–16, https://doi.org/10.1127/0372-8854/2007/0051s2-0001, 2007.

Haeberli, W.: Die Basis-Temperatur der winterlichen Schneedecke als möglicher Indikator für die Verbreitung von Permafrost in den Alpen, Zeitschrift für Gletscherkunde und Glazialgeologie, 9, 221–227, 1973.

Haeberli, W., Hallet, B., Arenson, L., Elconin, R., Humlum, O., Kääb, A., Kaufmann, V., Ladanyi, B., Matsuoka, N., Springman, S., and Mühll, D.V.: Permafrost creep and rock glacier dynamics, Permafrost Periglac., 17, 189–214, https://doi.org/10.1002/ppp.561, 2006.

Hartl, L., Zieher, T., Bremer, M., Stocker-Waldhuber, M., Zahs, V., Höfle, B., Klug, C., and Cicoira, A.: Multi-sensor monitoring and data integration reveal cyclical destabilization of the Äußeres Hochebenkar rock glacier, Earth Surf. Dynam., 11, 117–147, https://doi.org/10.5194/esurf-11-117-2023, 2023.

Hauck, C., Böttcher, M., and Maurer, H.: A new model for estimating subsurface ice content based on combined electrical and seismic data sets, The Cryosphere, 5, 453–468, https://doi.org/10.5194/tc-5-453-2011, 2011.

Hausmann, H., Krainer, K., Brückl, E., and Mostler, W.: Internal structure and ice content of Reichenkar rock glacier (Stubai Alps, Austria) assessed by geophysical investigations, Permafrost Periglac., 18, 351–367, https://doi.org/10.1002/ppp.601, 2007.

Hawker, L., Uhe, P., Paulo, L., Sosa, J., Savage, J., Sampson, C., and Neal, J.: A 30 m global map of elevation with forests and buildings removed.Environ.Res.Lett., 17(2), 2022.

Herring, T., Lewkowicz, A. G., Hauck, C., Hilbich, C., Mollaret, C., Oldenborger, G. A., Uhlemann, S., Farzamian, M., Calmels, F., and Scandroglio, R.: Best practices for using electrical resistivity tomography to investigate permafrost, Permafrost Periglac., 34, 494-512, https://doi.org/10.1002/ppp.2207, 2023.

Hoelzle, M.: Permafrost occurrence from BTS measurements and climatic parameters in the eastern Swiss Alps, Permafrost Periglac., 3, 143–147, https://doi.org/10.1002/ppp.3430030212, 1992.

Hoelzle, M., Wegmann, M., and Krummenacher, B.: Miniature temperature dataloggers for mapping and monitoring of permafrost in high mountain areas: First experience from the Swiss Alps, Permafrost Periglac., 10, 113–124, 10.1002/(SICI)1099-1530(199904/06)10:23.0.CO;2-A, 1999.

Hu, Y., Arenson, L. U., Barboux, C., Bodin, X., Cicoira, A., Delaloye, R., Gärtner-Roer, I., Kääb, A., Kellerer-Pirklbauer, A., Lambiel, C., Liu, L., Pellet, C., Rouyet, L., Schoeneich, P., Seier, G., and Strozzi, T.: Rock glacier velocity: An Essential Climate Variable Quantity for Permafrost, Rev. Geophys., 63(1), e2024RG000847, https://doi.org/10.1029/2024RG000847, 2025.

Ishikawa, M., Fukui, K., Aoyama, M., Ikeda, A., Sawada, Y., and Matsuoka, N.: Mountain permafrost in Japan: Distribution, landforms and thermal regimes, Z. Geomorphol. Supp., 130, 99–116, 2003.

Kääb, A., Frauenfelder, R. and Roer, I.: On the response of rockglacier creep to surface temperature increase, Glob. Planet. Change, 56, 172-187, https://doi.org/10.1016/j.gloplacha.2006.07.005, 2007.

Kääb, A., Strozzi, T., Bolch, T., Caduff, R., Trefall, H., Stoffel, M., and Kokarev, A.: Inventory and changes of rock glacier creep speeds in Ile Alatau and Kungöy Ala-Too, northern Tien Shan, since the 1950s, The Cryosphere, 15, 927–949, https://doi.org/10.5194/tc-15-927-2021, 2021.

Kääb, A. and Røste, A.: Rock glaciers across the United States predominantly accelerate coincident with rise in air temperatures, Nat. Commun., 15, 7581, https://doi.org/10.1038/s41467-024-52093-z, 2024.

Kellerer-Pirklbauer, A., Wangensteen, B., Farbrot, H., and Etzelmüller, B.: Relative surface age-dating of rock glacier systems near Hólar in Hjaltadalur, northern Iceland, J. Quaternary Sci., 23, 137–151, https://doi.org/10.1002/jqs.1117, 2008.

Kellerer-Pirklbauer, A., Lieb, G.K., and Kleinferchner, H.: A new rock glacier inventory of the eastern European Alps, Austrian J. Earth Sci., 105, 78–93, 2012.

Kellerer-Pirklbauer, A.: Long-term monitoring of sporadic permafrost at the eastern margin of the European Alps (Hochreichart, Seckauer Tauern range, Austria), Permafrost Periglac., 30, 260–277, https://doi.org/10.1002/ppp.2021, 2019.

Kellerer-Pirklbauer, A., Lieb, G.K., Kaufmann, V.: Rock Glaciers in the Austrian Alps: A General Overview with a Special Focus on Dösen Rock Glacier, Hohe Tauern Range. In: Embleton-Hamann, C. (eds) Landscapes and Landforms of Austria. World Geomorphological Landscapes. Springer, Cham, pp. 393–406, https://doi.org/10.1007/978-3-030-92815-5_27, 2022.

Kellerer-Pirklbauer, A., Bodin, X., Delaloye, R., Lambiel, C., Gärtner-Roer, I., Bonnefoy-Demongeot, M., Carturan, L., Damm, B., Eulenstein, J., Fischer, A., Hartl, L., Ikeda, A., Kaufmann, V., Krainer, K., Matsuoka, N., Di Cella, U.M., Noetzli, J., Seppi, R., Scapozza, C., Schoeneich, P., Stocker-Waldhuber, M., Thibert, E., and Zumiani, M.: Acceleration and interannual variability of creep rates in mountain permafrost landforms (rock glacier velocities) in the European Alps in 1995-2022, Environ. Res. Lett., 19, 034022, https://doi.org/10.1088/1748-9326/ad25a4, 2024.

Kenner, R., Pruessner, L., Beutel, J., Limpach, P., and Phillips, M.: How rock glacier hydrology, deformation velocities and ground temperatures interact: Examples from the Swiss Alps, Permafrost Periglac., 31, 3–14, https://doi.org/10.1002/ppp.2023, 2020.

LAKI II MNT: Agentia Nationala de Cadastru si Publicitate Imobiliara: Land Administration Knowledge Improvement, available online: geoportal.ancpi.ro last acces: 01.09.2024, 2024.

Lambiel, C., Strozzi, T., Paillex, N., Vivero, S., and Jones, N.: Inventory and kinematics of active and transitional rock glaciers in the Southern Alps of New Zealand from Sentinel-1 InSAR, Arctic Antarct. Alp. Res., 55, 2183999, https://doi.org/10.1080/15230430.2023.2183999, 2023.

Lilleøren, K.S., Etzelmüller, B., Rouyet, L., Eiken, T., Slinde, G., and Hilbich, C.: Transitional rock glaciers at sea level in northern Norway, Earth Surf. Dynam., 10, 975–996, https://doi.org/10.5194/esurf-10-975-2022, 2022.

Liu, L., Millar, C.I., Westfall, R.D., and Zebker, H.A.: Surface motion of active rock glaciers in the Sierra Nevada, California, USA: Inventory and a case study using InSAR, The Cryosphere, 7, 1109–1119, https://doi.org/10.5194/tc-7-1109-2013, 2013.

Marcer, M., Cicoira, A., Cusicanqui, D., Bodin, X., Echelard, T., Obregon, R., and Schoeneich, P.,: Rock glaciers throughout the French Alps accelerated and destabilised since 1990 as air temperatures increased, Commun. Earth Environ., 2, https://doi.org/10.1038/s43247-021-00150-6, 2021.

Mollaret, C., Wagner, F.M., Hilbich, C., Scapozza, C., and Hauck, C.: Petrophysical Joint Inversion Applied to Alpine Permafrost Field Sites to Image Subsurface Ice, Water, Air, and Rock Contents, Front. Earth Sci., 8, 85, https://doi.org/10.3389/feart.2020.00085, 2020.

Necsoiu, M., Onaca, A., Wigginton, S., and Urdea, P.: Rock glacier dynamics in Southern Carpathian Mountains from high-resolution optical and multi-temporal SAR satellite imagery, Remote Sens. Environ., 177, 21–36, https://doi.org/10.1016/j.rse.2016.02.025, 2016.

Oliva, M., Fernandes, M., Palacios, D., Fernández-Fernández, J.M., Schimmelpfennig, I., Antoniades, D., Aumaître, G., Bourlès, D., and Keddadouche, K.: Rapid deglaciation during the Bølling-Allerød Interstadial in the Central Pyrenees and associated glacial and periglacial landforms, Geomorphology, 385, 107735, https://doi.org/10.1016/j.geomorph.2021.107735, 2021.

Onaca, A.L., Urdea, P., and Ardelean, A.C.: Internal structure and permafrost characteristics of the rock glaciers of Southern Carpathians (Romania) assessed by geoelectrical soundings and thermal monitoring, Geogr. Ann. A., 95, 249–266, https://doi.org/10.1111/geoa.12014, 2013.

Onaca, A., Ardelean, A.C., Urdea, P., Ardelean, F., and Sirbu, F.: Detection of mountain permafrost by combining conventional geophysical methods and thermal monitoring in the Retezat Mountains, Romania, Cold Reg. Sci. Technol., 119, 111–123, https://doi.org/10.1016/j.coldregions.2015.08.001, 2015.

Onaca, A., Urdea, P., Ardelean, A.C., Șerban, R., and Ardelean, F.: Present-day periglacial processes in the alpine zone, in: Landform Dynamics and Evolution in Romania, edited by: Rădoane, M., Vespremeanu-Stroe, A., Springer Geography, 147-176, 2017a.

Onaca, A., Ardelean, F., Urdea, P., and Magori, B.: Southern Carpathian rock glaciers: Inventory, distribution and environmental controlling factors, Geomorphology, 293, 391-404, http://dx.doi.org/10.1016/j.geomorph.2016.03.032, 2017b.

Onaca, A., Ardelean, F., Ardelean, A., Magori, B., Sîrbu, F., Voiculescu, M., and Gachev, E.: Assessment of permafrost conditions in the highest mountains of the Balkan Peninsula, Catena, 185, 104288, https://doi.org/10.1016/j.catena.2019.104288, 2020.

Noetzli, J., Isaksen, K., Christiansen, H., Delaloye, R., Etzelmüller, B., Farinotti, D., Gallemann, T., Guglielmin, M., Hauck, C., Hilbich, C., Hoelzle, M., Lambiel, C., Magnin, F., Oliva, M., Paro, L., Pogliotti, P., Riedl, C., Schoeneich, P., Valt, M., Vieli, M., and Philips, M.: Enhanced warming of European mountain permafrost in the early 21st century, Nat. Commun., 15, 10508, https://doi.org/10.1038/s41467-024-54831-9, 2024.

Pavelescu, L.: Studiu geologic și petrografic al regiunii centrale și de sud-est a Munților Retezat [Geological and petrographic study of the central and south-eastern region of the Retezat Mountains], AIGR, XXV, 119-210, 1953.

Pandey, P., Nawaz Ali, S., Subhasmita Das, S., and Ataullah Raza Khan, M.: Rock glaciers of the semi-arid northwestern Himalayas: distribution, characteristics, and hydrological significance, Catena, 238, 107845, https://doi.org/10.1016/j.catena.2024.107845, 2024.

Pellet, C., Bodin, X., Cusicanqui, D., Delaloye, R., Kääb, A., Kaufmann, V., Thibert, E., Vivero, S., and Kellerer-Pirklbauer, A.: Rock glacier velocity. In: State of the Climate in 2023, Bull. Am. Meteorol. Soc., 105, 44–46, https://doi.org/10.1175/2024BAMSStateoftheClimate.1, 2024.

Poncoș, V., Stanciu, I., Teleagă, D., Mațenco, L., Bozsó, I., Szakács, A., Birtas, D., Toma, Ș.A., Stănică, A., and Rădulescu, V.: An Integrated Platform for Ground-Motion Mapping, Local to Regional Scale; Examples from SE Europe, Remote Sens-Basel., 14, 1046, https://doi.org/10.3390/rs14041046, 2022.

Popescu, R., Vespremeanu-Stroe, A., Onaca, A., and Cruceru, N.: Permafrost research in the granitic massifs of Southern Carpathians (Parâng Mountains), Z. für Geomorphol, 59(1), 1-20, doi.org/10.1127/0372-8854/2014/0145, 2015.

Popescu, R., Onaca, A., Urdea, P., and Vespremeanu-Stroe, A.: Spatial Distribution and Main Characteristics of Alpine Permafrost from Southern Carpathians, Romania, In Rădoane, M., Vespremeanu-Stroe, A. (Eds.), Landform dynamics and evolution in Romania, Springer, 117-146, DOI: 10.1007/978-3-319-32589-7_6, 2017.

Popescu, R., Filhol, S., Etzelmüller, B., Vasile, M., Pleșoianu, A., Vîrghileanu, M., Onaca, A., Șandric, I., Săvulescu, I., Cruceru, N., Vespremeanu-Stroe, A., Westermann, S., Sîrbu, F., Mihai, B., Nedelea, A., and Gascoin, S.: Permafrost Distribution in the Southern Carpathians, Romania, Derived From Machine Learning Modeling, Permafrost Periglac., 35, 243–261, https://doi.org/10.1002/ppp.2232, 2024.

Rangecroft, S., Harrison, S., and Anderson, K.: Rock glaciers as water stores in the Bolivian Andes: An assessment of their hydrological importance, Arct. Antarct. Alp. Res., 47, 89–98, https://doi.org/10.1657/AAAR0014-029, 2015.

RGIK: Guidelines for inventorying rock glaciers: baseline and practical concepts (version 1.0). IPA Action Group Rock glacier inventories and kinematics, 25, DOI:10.51363/unifr.srr.2023.002, 2023a.

RGIK: InSAR-based kinematic attribute in rock glacier inventories. Practical InSAR Guidelines (version 4.0., 31.05.2023), IPA Action Group Rock Glacier Inventories and Kinematics (RGIK), 33 pp, www.rgik.org, 2023b.

Roer, I., Haeberli, W., Avian, M., Kaufmann, V., Delaloye, R., Lambiel, C., and Kääb, A.: Observations and considerations on destabilizing active rock glaciers in the European Alps, in: Proc. Ninth Int. Conf. on Permafrost, Fairbanks, Alaska, 29 June–3 July 2008, Kane, D. L. and Hinkel, K. M. (Eds.), Institute of Northern Engineering, University of Alaska, pp. 1505–1510, 2008.

Rouyet, L., Lilleoren, K.S., Boehme, M., Vick, L.M., Delaloye, R., Etzelmüller, B., Lauknes, T.R., Larsen, Y., and Blikra, L.H.: Regional Morpho-Kinematic Inventory of Slope Movements in Northern Norway, Front. Earth Sci. 9, 681088, https://doi.org/10.3389/feart.2021.681088, 2021.

Rucci, A., Ferretti, A., Monti Guarnieri, A., and Rocca, F.: Sentinel 1 SAR interferometry applications: The outlook for sub millimeter measurements, Remote Sens. Environ., 120, 156–163, https://doi.org/10.1016/j.rse.2011.09.030, 2012.

Rücker, C., Günther, T., and Wagner, F.M.: pyGIMLi: An open-source library for modelling and inversion in geophysics, Comput. Geosci., 109, 106–123, https://doi.org/10.1016/j.cageo.2017.07.011, 2017.

Ruszkiczay-Rüdiger, Z., Kern, Z., Urdea, P., Madarász, B., Braucher, R., and ASTER Team: Limited glacial erosion during the last glaciation in mid-latitude cirques (Retezat Mts, Southern Carpathians, Romania), Geomorphology, 384, 107719, https://doi.org/10.1016/j.geomorph.2021.107719, 2021.

Sandmeier, K.-J.: REFLEXW Version 9.1.3. Windows™ XP/7/8/10-program for the processing of seismic, acoustic or electromagnetic reflection, refraction and transmission data, 2020.

Santos-González, J., González-Gutiérrez, R.B., Redondo-Vega, J.M., Gómez-Villar, A., Jomelli, V., Fernández-Fernández, J.M., Andrés, N., García-Ruiz, J.M., Peña-Pérez, S.A., Melón-Nava, A., Oliva, M., Álvarez-Martínez, J., Charton, J., ASTER Team, and Palacios, D.: The origin and collapse of rock glaciers during the Bølling-Allerød interstadial: A new study case from the Cantabrian Mountains (Spain), Geomorphology, 401, 108112, https://doi.org/10.1016/j.geomorph.2022.108112, 2022.

Sattler, K., Anderson, B., Mackintosh, A., Norton, K., and de Róiste, M.: Estimating permafrost distribution in the maritime Southern Alps, New Zealand, based on climatic conditions at rock glacier sites, Front. Earth Sci., 4, 4, https://doi.org/10.3389/feart.2016.00004, 2016.

Schoeneich, P.: Guide lines for monitoring GST – Ground surface temperature, PERMANET project, Version 3 – 2.2.2011, https://www.permanet-alpinespace.eu/archive/pdf/GST.pdf, 2011, accessed 20 April 2025.

Scotti, R., Brardinoni, F., Alberti, S., Frattini, P., and Crosta, G.B.: A regional inventory of rock glaciers and protalus ramparts in the central Italian Alps, Geomorphology, 186, 136–149, https://doi.org/10.1016/j.geomorph.2012.12.028, 2013.

Serrano, E., de Sanjosé, J.J., and González-Trueba, J.J.: Rock glacier dynamics in marginal periglacial environments, Earth Surf. Proc. Land., 35, 1302–1314, https://doi.org/10.1002/esp.1972, 2010.

Steinemann, O., Reitner, J.M., Ivy-Ochs, S., Christl, M., and Synal, H.-A.: Tracking rockglacier evolution in the Eastern Alps from the Lateglacial to the early Holocene, Quaternary Sci. Rev., 241, 106424, https://doi.org/10.1016/j.quascirev.2020.106424, 2020.

Stiegler, C., Rode, M., Sass, O., and Otto, J.C.: An Undercooled Scree Slope Detected by Geophysical Investigations in Sporadic Permafrost below 1000 M ASL, Central Austria, Permafrost Periglac., 25, 194–207, https://doi.org/10.1002/ppp.1813, 2014.

Strozzi, T., Caduff, R., Jones, N., Barboux, C., Delaloye, R., Bodin, X., Kääb, A., Mätzler, E., and Schrott, L.: Monitoring rock glacier kinematics with satellite synthetic aperture radar, Remote Sens-Basel., 12, 559, https://doi.org/10.3390/rs12030559, 2020.

Timur, A.: Velocity of compressional waves in porous media at permafrost temperatures, Geophysics, 33, 584–595, https://doi.org/10.1190/1.1439954, 1968.

Urdea, P.: Permafrost and periglacial forms in the Romanian Carpathians, in: 6th International Conference on Permafrost, South China University of Technology, Beijing, China, 631–637, 1993.

Urdea, P.: Munţii Retezat, Studiu geomorfologic [Retezat Mountains. A geomorphological study], Academiei, Bucureşti, 272 pp, ISBN 973-27-0767-4, 2000.

893   Vespremeanu-Stroe, A., Urdea, P., Popescu, R., and Vasile, M.: Rock Glacier Activity in the Retezat Mountains, Southern
894   Carpathians, Romania, Permafrost Periglac., 23, 127–137, https://doi.org/10.1002/ppp.1736, 2012.

895   Vonder Mühll, D., Hauck, C., and Gubler, H.: Mapping of mountain permafrost using geophysical methods, Prog. Phys. Geog.,
896   26, 643–660, https://doi.org/10.1191/0309133302pp356ra, 2002.

897   Wagner, F.M., Mollaret, C., Günther, T., Kemna, A., and Hauck, C.: Quantitative imaging of water, ice and air in permafrost
898   systems through petrophysical joint inversion of seismic refraction and electrical resistivity data, Geophys. J. Int., 219, 1866–
899   1875, https://doi.org/10.1093/gji/ggz402, 2019.

900   Wagner, T., Seelig, S., Helfricht, K., Fischer, A., Avian, M., Krainer, K., and Winkler, G.: Assessment of liquid and solid
901   water storage in rock glaciers versus glacier ice in the Austrian Alps, Sci. Total Environ., 800, 149593,
902   https://doi.org/10.1016/j.scitotenv.2021.149593, 2021.

903   Wicky, J. and Hauck, C.: Numerical modelling of convective heat transport by air flow in permafrost talus slopes, The
904   Cryosphere, 11, 1311-1325, https://doi.org/10.5194/tc-11-1311-2017, 2017.

905   Wirz, V., Gruber, S., Purves, R.S., Beutel, J., Gärtner-Roer, I., Gubler, S., and Vieli, A.: Short-term velocity variations at three
906   rock glaciers and their relationship with meteorological conditions, Earth Surf. Dynam., 4, 103–123,
907   https://doi.org/10.5194/esurf-4-103-2016, 2016.

908   Yu, J., Meng, X., Yan, B., Xu, B., Fan, Q., and Xie, Y.: Global Navigation Satellite System-based positioning technology for
909   structural health monitoring: a review, Struct. Control. Hlth., 27, 2467, https://doi.org/10.1002/stc.2467, 2020.

910